



UNIVERSITÀ DEGLI STUDI DI TRIESTE

Dipartimento Universitario Clinico di Scienze Mediche, Chirurgiche e della Salute

XXIX CICLO DEL DOTTORATO DI RICERCA IN SCIENZE DELLA RIPRODUZIONE E DELLO SVILUPPO

Identification of new Hereditary Hearing Loss genes using High-Throughput Sequencing Technologies

Settore scientifico-disciplinare: **MED03**

Ph.D Student:

Anna Morgan

Ph.D program Coordinator:

Prof. Alessandro Ventura

Thesis Supervisor:

Prof. Paolo Gasparini

Thesis Co-supervisor:

Dr. Giorgia Girotto

ANNO ACCADEMICO 2015-2016

CONTENTS

ABSTRACT	4
1. INTRODUCTION	6
1.1 The Anatomy of the Ear and the Auditory Transduction	6
1.1.1 The Outer Ear.....	6
1.1.2 The Middle Ear	7
1.1.3 The Inner Ear	7
1.1.3.1 Cochlear Structure.....	7
1.1.3.2 Organ of Corti.....	9
1.1.4 Auditory Transduction	11
1.2 Hearing Impairment and Loss	12
1.2.1 Syndromic Hearing Impairment and Loss	14
1.2.2 Non Syndromic Hearing Impairment and Loss.....	14
1.2.3 Genes and Proteins related to NSHI/NSHL.....	15
1.2.3.1 Ion Homeostasis and Gap Junctions.....	15
1.2.3.2 Adhesion Proteins.....	17
1.2.3.3 Transport Proteins	18
1.2.3.4 Protein of synapses	18
1.2.3.5 Cytoskeleton.....	18
1.2.3.6 Electromotility.....	19
1.2.3.7 Other	20
1.3 Next Generation Sequencing.....	20
2. AIMS OF THE STUDY	23
3. MATERIALS AND METHODS	24
3.1 Patients Selection and Recruitment	24
3.2 DNA Isolation and Quality Control.....	25
3.3 Targeted re-Sequencing (TRS)	25
3.3.1 Custom TRS Panel	25
3.3.2 Library Preparation	28
3.3.3 Template Preparation and Sequencing	28
3.4 Whole Exome Sequencing (WES)	29
3.5 Data Analysis	30
3.6 Functional Validation	32
3.6.1 Protein Modelling.....	32

3.6.2 <i>In vitro</i> Molecular Cloning	34
3.6.2.1 Western Blot Analysis	34
3.6.2.2 Quantitative Real-Time PCR (qRT-PCR)	35
3.6.3 <i>In vivo</i> expression studies.....	35
3.6.3.1. Gene expression in mouse tissues	35
3.6.3.2. Gene expression in Zebrafish larvae.....	36
4. RESULTS AND DISCUSSION	38
4.1 Patients.....	38
4.2 Targeted Resequencing (TRS)	38
4.3 Whole Exome Sequencing (WES)	47
4.3.1 <i>SPATC1L</i>	47
4.3.1 <i>PLS1</i>	55
5. CONCLUSIONS.....	60
6. REFERENCES.....	62

ABSTRACT

Hearing impairment (HI) and hearing loss (HL) are the most frequent birth defects in developed societies affecting approximately 1 to 3 in every 1000 live births. HI/HL are remarkably complex and heterogeneous diseases presenting with various phenotypes as a result of both genetic and environmental factors. Within genetic or hereditary hearing impairment/loss (HHI/HHL) about 70% of cases can be classified as non-syndromic (NSHI/NSHL), i.e. with the absence of abnormalities in other organs, and to date 158 NSHI/NSHL loci and 95 genes have been reported as causative.

Considering that the achievement of a correct molecular diagnosis is essential for uncovering the molecular mechanisms of hearing loss, in order to provide patients with prognostic information and personalized risk assessments and reduce public health costs, this study aims to define the genetic cause of deafness in a subset of NSHI/NSHL familial cases coming from both Italy and Qatar.

In order to overcome the high genetic heterogeneity of this disease and the fact that different major players seem to be involved in the Italian and Qatari populations, next generation sequencing techniques have been employed in this study.

In particular, in the case of the Qatari population, this work represents the first high-throughput screening for the molecular diagnosis of hearing loss, being thus extremely valuable from an epidemiological point of view.

As a first step, patients have been screened for 96 deafness-genes using a custom targeted re-sequencing (TRS) panel. Data analysis led to the identification of the molecular cause in 50% of all families, highlighting *TECTA* and *MYO7A* as major players in the Italian population, and *CDH23* and *TMC1* in the Qatari one.

.

Families negative to TRS have been selected for whole exome sequencing (WES) analysis, with the purpose of discovering new disease-related genes. So far two new candidates, *SPATC1L* and *PLS1*, in two Italian families have been identified.

SPATC1L encodes the speriolin-like protein, whose function is still unknown. A novel stop variant has been identified in an Italian family affected by autosomal dominant NSHL (ADNSHL) and some functional studies (i.e. expression analysis in mouse whole cochleae, protein modelling and *in vitro* molecular cloning) together with statistical analysis (i.e. a candidate-gene population-based statistical study in cohorts from Caucasus and Central Asia) supported the role of this gene in hearing function and loss.

In the case of *PLS1*, a new missense variant has been identified in an Italian ADNSHL family. The gene encodes the plastin-1 protein, which has already been associated to hearing loss in mice. The generation of a knock-in in Zebrafish model (in collaboration with ZeClinics, a Biotech Contract Research Organization (CRO) and early-phase biopharmaceutical (PHARMA) company that uses Zebrafish for the study of human diseases, located in Barcelona, Spain) is now in progress and gene expression in Zebrafish larvae inner ear has been preliminary confirmed.

Altogether these results clearly proved that TRS followed by WES and functional studies are powerful tools for both the molecular diagnosis of NSHI/NSHL, and the identification of new disease-related genes.

1. INTRODUCTION

1.1 The Anatomy of the Ear and the Auditory Transduction

The ear is the primary organ of the auditory system, which plays a fundamental role in both detecting sound and positioning and balancing of the body.

The ear consists of three sections: the outer ear, the middle ear and the inner ear (**Figure 1.1**) that altogether are essential for the mechanism of sound transduction.

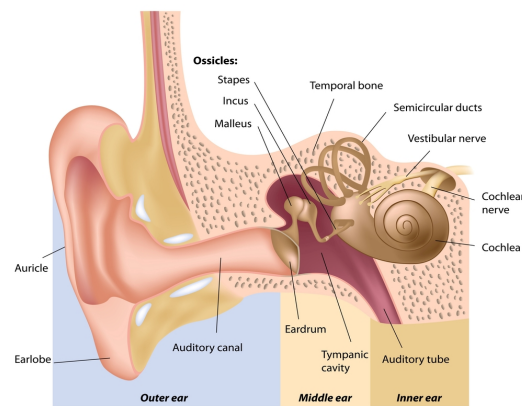


Figure 1.1 Schematic representation of the auditory system. The mammalian ear is made up of three distinct sections: the outer ear, the middle ear and inner ear. The outer ear consists of the auricle, the auditory canal and the eardrum, that marks the beginning of the middle ear. The middle ear contains the malleus, incus and stapes, the auditory ossicles. The inner ear consists of the cochlear and the vestibular system (adapted from *"The human ear facts and functions of the ear -an organ of hearing"* <http://www.organsofthebody.com/ears/>).

1.1.1 The Outer Ear

The outer ear is the external portion of the ear and essentially acts as a resonator enhancing the transmission of sound waves (1).

It is made up of the auricle (also called pinna), the external auditory canal and the eardrum, the most superficial layer of the tympanic membrane.

The auricle collects sound waves and canalises them to the eardrum via the auditory canal. Vibration of the tympanic membrane represents the first stage of the sound transduction pathway.

1.1.2 The Middle Ear

The middle ear is an air-filled cavity enclosed by the temporal bone and interposed between the eardrum and the oval window, a membrane-covered opening that connects the middle ear to the inner ear.

The middle ear contains three small bones, also known as the ossicles: the malleus (hammer), incus (anvil) and stapes (stirrup).

These bones form the ossicular chain that allows amplifying and transferring the sound-induced vibrations of the tympanic membrane to the inner ear via a connection between the stapes footplate and the oval window (2).

1.1.3 The Inner Ear

The inner ear is a fluid-filled cavity located in the temporal bone.

It consists of the cochlea, the auditory sense organ, and the vestibular system, which is required for balance (3).

Vibrations of the tympanic membrane are transferred via the ossicles chain to the cochlea, where the mechanical stimuli are converted into electrical signals that can travel along the eighth cranial nerve to the brain allowing auditory perception.

1.1.3.1 Cochlear Structure

The cochlea is a fluid-filled coiled structure spiralled around a central bone called the modiolus. The cochlear duct is divided from the vestibular membrane (also known as

Reissner's membrane) and the basilar membrane in three fluid-filled chambers (or scalae): scala vestibuli, scala media and scala tympani (**Figure 1.2**).

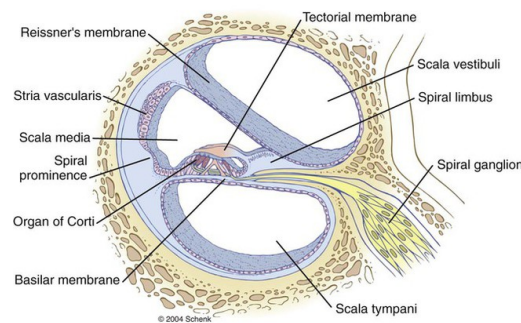


Figure 1.2 Diagram of a cross section of the cochlea. The cochlea is divided from the Reissner's membrane and basilar membrane into three fluid-filled sections, named scala vestibuli, scala media and scala tympani (adapted from Guyton and Hall, *Textbook of medical physiology*, ed 12, Philadelphia, 2011, Saunders).

The two outer sections of the cochlear duct are the scala vestibuli, which is connected to the oval window, and the scala tympani, which is connected to the round window, the second opening from the middle ear into the inner ear, sealed by the round window membrane. Although separated along the length of the cochlea, these two scalae meet at the apex, in a region called helicotrema, thus forming a continuous duct that surrounds the third section, the scala media.

Both the scala vestibuli and the scala tympani are filled with a fluid known as perilymph, which is an extracellular-like fluid, with high concentration of sodium (150 mM), and low concentration of potassium (5 mM) (4).

The scala media is the third compartment of the cochlea. It is a triangular-shaped duct filled with endolymph. The endolymph shows an ionic composition very similar to that of an intracellular fluid, i.e. it is high in potassium (150 mM) and in low sodium (5 mM) and calcium (0.02 mM) (while the perilymph has a higher calcium concentration of about 1 mM) (4).

Furthermore, this solution exhibits an endocochlear potential (EP) of +80 mV with respect to the perilymph (5).

The scala media houses the organ of Corti, the receptor organ for hearing, where the auditory transduction takes place.

1.1.3.2 Organ of Corti

The organ of Corti consists of an array of mechanosensory cells, known as hair cells, and different types of supporting cells (**Figure 1.3**).

Hair cells are distributed in rows along the length of the cochlea and can be classified in inner hair cells (IHCs), and outer hair cells (OHCs). In particular, a single row of IHCs and three rows of OHCs sit on the basilar membrane, anchored by a series of supporting cells.

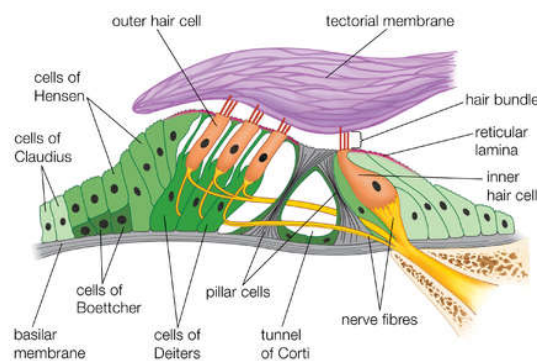


Figure 1.3 Schematic representation of the organ of Corti. The organ of Corti contains a sensory epithelium, which sits on top of the basilar membrane, made of sensory cells known as hair cells. Three rows of outer hair cells and one row of inner hair cells, surrounded by supporting cells, are present. The tectorial membrane is a collagen rich extracellular matrix that lies on top of the hair cells and makes contact with the stereocilia, specialised actin-rich structures essential for the auditory transduction (adapted from “*Encyclopaedia Britannica*” <https://www.britannica.com/science/organ-of-Corti>).

On the apical surface of the hair cells are specialised structures known as stereocilia.

Stereocilia are actin-rich organelles that project out into the endolymph and are essential for the auditory transduction.

Stereocilia are usually arranged in bundles of approximately 20-300 units (6). Within these bundles stereocilia are lined up in rows of increasing height, similar to a staircase, in which a row of shorter stereocilia is connected to the next row of taller stereocilia by tip links. There are also additional connecting links, known as lateral links, between stereocilia by tip links. There are also additional connecting links, known as lateral links. (Figure 1.4.A)

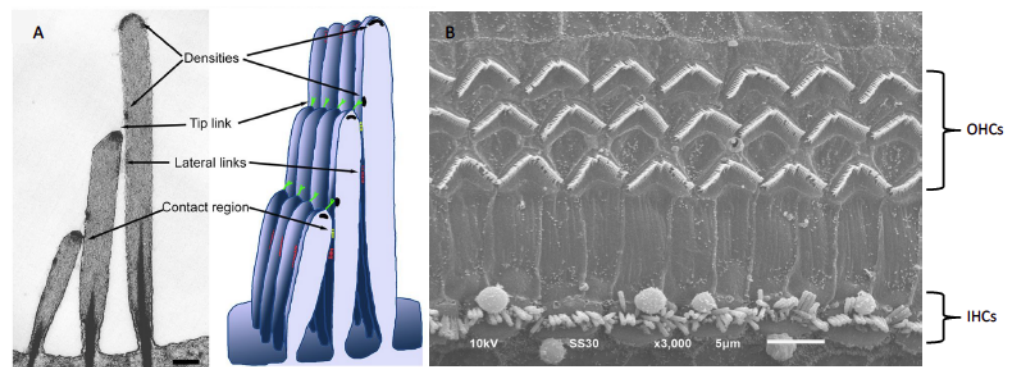


Figure 1.4 Stereocilia organization. (A) Stereocilia are actin rich structures which protrude from the apex of hair cells. They are organized in bundles, formed with several rows of stereocilia in increasing height. Tip links connect the apex of the stereocilia in adjacent bundles and in addition, there are lateral links along the length of the stereocilia. (B) A scanning electron micrograph (SEM) showing stereocilia arrangement in the cochlea. There are three rows of OHCs and one row of IHCs. Stereocilia bundle of OHCs shows the characteristic V shaped, whereas stereocilia of IHCs show a more linear pattern (adapted from Hackney and Furness, *"The composition and role of cross links in mechanoelectrical transduction in vertebrate sensory hair cells"*, J Cell Sci 2013 126: 1721-1731; doi: 10.1242/jcs.106120).

Stereocilia are embedded in a gelatinous structure called tectorial membrane, an extracellular matrix which extends along the length of the cochlea in parallel to the basilar membrane overlying the OHCs and the IHCs

1.1.4 Auditory Transduction

As previously mentioned, in response to an auditory stimulus, sound waves enter the outer ear and propagate along the auditory canal to the eardrum, causing it to vibrate. Vibration of the tympanic membrane triggers the movement of the ossicles chain. In particular, the malleus, which is attached to the tympanic membrane on one end and to the incus on the other, causes the movement of the incus that in turn is connected to the stapes. Thus, the footplate of the stapes presses against the oval window inducing a change in pressure within the inner ear.

The stapes-induced pressure waves propagate along the scala vestibuli and the scala tympani, exiting via the round window, and results in the vibration of the basilar membrane.

The basilar membrane, a stiff membrane that extends along the length of the cochlea, divides the scala media from the scala tympani. It has different properties along its length: it is narrowest and stiffest at the base of the cochlea (closest to the oval window) and gets wider and less stiff towards the apical end. This gradient in physical properties determines the frequency at which the membrane is most sensitive to sound vibrations and it is known as tonotopic organisation (7). Oscillations of the basilar membrane cause the organ of Corti to rise up against the tectorial membrane. As a result stereocilia are sheared back and forth under the tectorial membrane. This movement causes the deflection of the hair bundle towards the tallest row and the stretching of the tip links that allows the opening of non-selective cation channels known as mechanotransduction (MET) channels (8).

The opening of MET channels as a result of stereocilia deflection therefore triggers K^+ to flood into the hair cells down a concentration gradient. This influx leads to cell depolarisation (9). Depolarization in turn opens voltage-gated calcium channels in the hair cell membrane, and the resultant Ca^{2+} influx causes transmitter (glutamate) release from the base of the cell to the auditory nerve endings.

Afferent neurons form synapses with IHCs and relay the electrical signals to the spiral ganglion neurons (SGN). These neurons transmit the signals, via the eighth cranial nerve, to the auditory centres of the brain.

On the other hand, OHCs behave as cochlea amplifiers responsible for sharpening the frequency-specific response of the cochlea and are innervated by efferent dendrites (10).

Repolarization of the hair cells takes place via K^+ efflux; the opening of MET channels in fact leads also to the activation of K^+ channels located in the membrane of the hair cell soma. The opening of somatic K^+ channels favors K^+ efflux (in fact the surrounding perilymph is low in K^+ relative to the cytosol). Moreover another avenue for K^+ to enter the perilymph and repolarize the cell is given by the opening of Ca^{2+} -dependent K^+ channels (9).

1.2 Hearing Impairment and Loss

Hearing impairment and loss (HI/HL) are the most frequent birth defect in developed societies, and congenital hearing impairment affects approximately 1 to 3 in every 1000 live births (11).

The term HI refers to all cases of congenital deafness, while with the term HL all cases of acquired hearing deficit are indicated.

Deafness is typically described based on its clinical presentation and can be classified by a number of different factors such as age of onset, severity, aetiology and pathobiology (**Table 1.1**).

Classification	Description
Aetiology	Genetic
	Acquired (environmental, e.g. prenatal or postnatal infections)
Presentation	Syndromic: HI/HL associated with additional clinical features (approximately 400 syndromes have been described where HL is associated with defects in other systems e.g. renal, ocular, endocrine, nervous and musculoskeletal)
	Non-syndromic: HI/HL is the only clinical abnormality
Laterality	Unilateral: one ear affected
	Bilateral: both ears affected
Onset	Congenital: HI is present at birth
	Pre-lingual: HI/HL is present before speech develops
	Post lingual: HI/HL occurs after the development of normal speech.
Type	Conductive HI/HL: abnormalities or damage of the external ear and/or the ossicles of the middle ear (i.e., otitis media, otosclerosis, tumours, impacted cerumen)
	Sensorineural HI/HL: malfunction of inner ear (i.e., cochlea)
	Mixed HI/HL: combination of conductive and sensorineural HI/HL
	Central auditory dysfunction: dysfunction or damage involving the eighth cranial nerve, the auditory brain stem or the cerebral cortex
Symmetry	Symmetric
	Asymmetric
Stability	Progressive
	Non progressive
	Fluctuating
Degree in Decibels (dB)	Mild: 26-40 dB
	Moderate: 41-55 dB
	Moderately severe: 56-70 dB
	Severe: 71-90 dB
	Profound: >90 dB
Frequencies affected	Low (<500 Hz)
	Middle (501-2000 Hz)
	High (>2000 Hz)
Configuration of the audiometric analysis	Sloping
	Flat
	Rising
	Midfrequency (cookie-bite)

Table 1.1: Audiometric and clinical aspects of hearing loss (12) (13) (14) (15) (16)

Fifty % to 70% of cases of HI/HL are attributable to genetic causes (17). Genetic causes of deafness can be further categorised as to whether the gene causes hearing impairment or loss associated with multiple clinical features (syndromic) or whether the hearing impairment or loss is the only clinical sign (non-syndromic).

1.2.1 Syndromic Hearing Impairment and Loss

The term syndromic hearing impairment/loss (SHI/SHL) refers to the manifestation of hearing deficit together with other abnormalities. To date, approximately 400 syndromes have been described where deafness is associated with defects in other systems e.g. renal, ocular, endocrine, nervous and musculoskeletal (11).

Two major classes of SHI/SHL have been described: SHI/SHL due to middle ear defects together with or without inner ear defects (e.g. Crouzon facial dysostosis, Stickler syndrome and Mucopolysaccharidoses) and SHI/SHL due to isolated inner ear defects (e.g. Usher, Pendred, Alport and Jervell and Lange Nielsen syndromes) (18).

1.2.2 Non Syndromic Hearing Impairment and Loss

Non-syndromic hearing impairment/loss (NSHI/NSHL) accounts for the vast majority of hereditary HI/HL cases and can be classified according to the inheritance pattern. In ~80% of cases inheritance is autosomal recessive (the hearing deficit is usually congenital, labelled as 'DFNB'), in the other ~20% of cases inheritance is autosomal dominant (usually with delayed onset, labelled as 'DFNA'). The rest of non-syndromic hearing impairment/loss is either X-linked or mitochondrial (<1%) (19).

To date, 158 NSHI/NSHL loci (60 DFNA loci, 88 DFNB loci, 6 X-linked loci, 2 modifier loci, 1 Y-linked locus and 1 locus for auditory neuropathy) and 95 genes (27 DFNA genes, 56 DFNB genes, 8 DFNA/DFNB genes and 4 X-linked genes) have been

reported as causative (Hereditary Hearing Loss Homepage; <http://hereditaryhearingloss.org/>).

The structure and physiology of the inner ear is in many ways unique and different from any other anatomical locations. This could explain why so many genes are thought to be involved in inner-ear function and why the ear is so sensitive to mutations at these loci.

1.2.3 Genes and Proteins related to NSHI/NSHL

Mutations in genes that control ionic homeostasis, adhesion of hair cells, neurotransmitter release, cytoskeleton of hair cells and intracellular transport can all lead to malfunction of the cochlea (20).

1.2.3.1 Ion Homeostasis and Gap Junctions

The cochlea contains two types of fluids, the perilymph and the endolymph, which differ in ion composition. This difference contributes to the generation of the endocochlear potential, necessary to drive mechanotransduction. It goes without saying that a correct ion homeostasis is essential for the maintenance of normal hearing function.

The process of ion homeostasis involves several tight junctions protein, such as claudin 14 (*CLDN14*), tricellulin (*MARVELD2/TRIC*), tight junction protein 2 (*TJP2*), a number of connexins (*GJB*'s), *KCNQ4* (*KCNQ4*), *ATP2B2* (*ATP2B2/PMCA2*), barttin (*BSND*) and pendrin (*SLC26A4*), all of which are related to NSHI and NSHL (19).

Tight junctions, by generating a seal between adjacent cells, create a barrier that limits the free diffusion of ions. As a consequence, the apical side of the hair cells and supporting cells is exposed to the endolymph, while the basolateral surface is bathed in a fluid with an ionic composition similar to that of the perilymph, which fills up the so-called space of Nuel (21). When tight junction proteins are absent or

dysfunctional this space might change in electric potential, as in DFNB29 (22), DFNB49 (23) and DFNA51 (24).

On the other hand gap junctions, which are channels that extend over two adjacent membranes, enable the exchange of various small molecules and ions.

They consist of specialised proteins called connexins, which are expressed in the supporting cells of the organ of Corti and the connective tissue of the spiral ligament (25) and are associated with the recycling of potassium ions needed for normal hearing.

Six connexins form a hexamerical assembly, known as connexon or hemichannel that can be homomeric (made of the same type of connexins), or heteromeric (made of different type of connexins). When two hemichannels from adjacent cells dock and join they form an intercellular gap junction channel (26).

In the Caucasian population mutations in *GJB2* gene, which encodes connexin 26, are the most common cause of recessive NSHI (DFNB1a) (even though *GJB2* has also been associated to autosomal dominant hearing loss, DFNA3a) (27). In particular, mutations in *GJB2* account for 30–50% of all congenital NSHI cases, and 1–4% of the average human population are estimated to be carriers (28). Other connexins associated with non-syndromic hearing impairment and loss, are connexin 31 (*GJB3*, DFNA2b/DFNB91) and connexin 30 (*GJB6*, DFNA3b/DFNB1b). In particular, connexin 30 can assembly with connexin 26 in heteromeric connexons and it has been shown that *GJB6* deletions together with in trans *GJB2* heterozygous mutation can cause NSHI (29).

Given the significant contribution of *GJB2* and *GJB6*, it is a common use to screen these two genes in patients affected by NSHI (16).

Other genes involved in cochlear ion homeostasis and causative of NSHI/NSHL are *KCNQ4*, that encodes a voltage-gated potassium channel of the outer hair cells, mutated in DFNA2a (30), and *ATP2B2/PMCA2*, that encodes a calcium pump that acts as modifier of DFNB12 (31).

Other two genes, *BSND* and *SLC26A4*, which encode barttin (a chloride channel subunit) and pendrin (an anion exchanger) respectively, are involved in both syndromic (i.e. Bartter syndrome and Pendred's syndrome) and non-syndromic deafness (32) (33).

1.2.3.2 Adhesion Proteins

Throughout their existence, hair cells stereocilia are linked and interconnected to the tectorial membrane by several adhesion proteins.

During the maturation of the hair bundle, a set of temporary links maintain stability (lateral links and ankle links) and in mature hair cells stereocilia are connected by tectorial attachment crowns, horizontal top connectors, and tip links (34).

To date, several genes related to the linking apparatus have been described. These include: *CEACAM16* (carcinogenic antigen-related cell adhesion molecule 16), *CDH23* (cadherin 23), *STRC* (stereocilin), *USH1C* (harmonin), *OTOA* (otoancorin), *PCDH15* (protocadherin 15), *WHRN* (whirlin), *TMHS* (tetraspan membrane protein), and *PTPRQ* (tyrosine phosphatase receptor Q) (19).

CDH23, *PCDH15*, *PTPRQ* and *TMHS* genes make up the transient lateral links, preventing stereocilia fusion during development (21). In mature hair cells, they become a main component of the tip links and act as a gate, channelling mechanotransduction and providing stability, taking a central role in auditory function.

Whirlin and harmonin are scaffolding proteins. Mutations in these proteins cause both autosomal recessive NSH/NSHL and Usher syndrome (35–38).

Stereocilin is an extracellular matrix protein that is thought to make up both horizontal top connectors and tectorial membrane attachment links, that allow the tallest stereocilia of the OHC to attach to the tectorial membrane (39). The attachment site, also known as attachment crown, is generally formed by

CEACAM16 (40). In a similar way, otoancorin attaches nonsensory cells to the tectorial membrane (41).

1.2.3.3 Transport Proteins

In the inner ear, all transport proteins belong to the unconventional myosin family (19). These proteins can bind actin cytoskeleton and, using ATP, can move forward along actin filaments. Seven unconventional myosins have been associated with hereditary deafness: myosin Ia (DFNA48), myosin IIIa (DFNB30), myosin VI (DFNA22/DFNB37), myosin VIIa (DFNA11/DFNB2), nonmuscle myosin heavy chain IX (DFNA17), nonmuscle myosin heavy chain XIV (DFNA4), and myosin XVa (DFNB3) (21). All these proteins have their own specific function in the inner ear.

1.2.3.4 Protein of synapses

Two main genes, encoding protein acting at a synaptic level, have been described as causative of NSHI/NSHL.

The first one is *SLC17A8*, which encodes the vesicular glutamate receptor VGLUT3. It plays a role in the inner hair cells' synapses and when mutated causes autosomal dominant hearing impairment/loss (42).

The second gene is *OTOF*, which encodes the otoferlin, a protein that works with myosin VI at the synaptic cleft of the IHC and plays a role in the calcium-dependent fusion of vesicles to the plasma membrane (43).

1.2.3.5 Cytoskeleton

Several genes involved in the organisation of the cytoskeleton can cause NSHI/NSHL, i.e. *ACTG1* (γ -actin), *DIAPH1* (diaphanous 1), *TRIOBP* (trio-binding protein), *TPRN* (taperin), *SMPX* (small muscle protein, X-linked), *ESPN* (espin) and *RDX* (radixin) (19).

Mutations in *ACTG1* can cause autosomal dominant hearing loss, DFNA20/26, interfering with the remodelling process of the actin filaments in the stereocilia. In fact, stereocilia are constantly undergoing actin polymerisation at the tip and depolymerisation at the base, and it is known that γ -actin functions as a building block of hair cell stereocilia (44).

The organisation and binding of γ -actin at the base (the so-called 'taper region') of stereocilia is regulated by *TRIOBP* gene, which is associated to DFNB28 (45). Another protein that localises at the taper region is the regulating protein taperin, which is associated with DFNB79 (46).

Together with γ -actin also diaphanous 1 protein is important in stereocilia remodelling process. In fact, *DIAPH1* regulates the polymerisation and reorganisation of actin monomers into polymers, and has been associated with DFNA1 (47).

The X-linked gene *SMPX* (DFN4) seems to have a function in stereocilial development and maintenance in response to the mechanical stress that they are subjected to (48).

The protein espin acts as a bundling protein, providing stability to the stereocilial cytoskeleton and when mutated causes DFNB3 and autosomal dominant hearing loss (49, 50).

More stability is provided by radixin, which is present along the length of the stereocilia and links actin filaments to the plasma membrane. Mutations in *RDX* cause recessive deafness, DFNB24 (51).

1.2.3.6 Electromotility

Electromotility is a process that guarantees an amplification of OHC sensitivity to sound by a shortening of the cell during depolarisation and a lengthening during hyper-polarisation.

It is thought that the protein Prestin, encoded by *SLC26A5*, is responsible for this mechanism, by changing its configuration in reaction to changes in membrane potential, enabling the outer hair cell length to be altered (52).

Mutations in *SLC26A5* are the cause of DFNB61 (53).

1.2.3.7 Other

Many other genes that do not belong to the categories above-mentioned can cause NSHI/NSHL. For instance, *TECTA* (α -tectorin), *COL11A2* (type XI collagen 2), *COCH* (cochlin), many transcription factors, such as *POU4F3* (class 4 POU), *POU3F4* (class 3 POU), *MIR96* (microRNA 96), *GRHL2* (grainy-head-like 2), *ESRRB* (oestrogen-related receptor), and *EYA4* (eyes absent 4) etc. (Hereditary Hearing Loss Homepage; <http://hereditaryhearingloss.org/>).

1.3 Next Generation Sequencing

The identification of the molecular cause of a Mendelian disorder is essential for proper genetic counselling, recurrence risk estimation, prognosis, and therapeutic options. However, in the case of NSHI/NSHL, the high genetic heterogeneity of the diseases has always made the definition of a molecular diagnosis really challenging. Moreover, predicting the specific causative gene for NSHI/NSHL based on the audiological phenotype is possible only for a few genes (e.g. *WFS1* (OMIM 606201), *COCH* (OMIM 603196), and *TECTA* (OMIM 602574)) (54).

The introduction of next generation sequencing (NGS) techniques has dramatically improved the diagnostic rate of non syndromic deafness, offering the opportunity to break through the barriers of limitations imposed by gene arrays and by a single-gene based analysis.

To date, due to the low throughput and cost-efficiency of Sanger sequencing, only few genes (e.g. *GJB2* (OMIM 121011), *SLC26A4* (OMIM 605646), and *OTOF* (OMIM 603681)) or specific mutations (e.g. *GJB6* deletions, *MTRNR1* mitochondrial mutations) are regularly analysed for autosomal-recessive NSHI (ARNSHI) in most routine diagnostic settings (55), alternatively NGS approaches are preferable.

So far, both Targeted Re-Sequencing (TRS) and Whole Exome Sequencing (WES) have been applied for the study of NSHI/NSHL (56, 57).

With TRS, a subset of genes or regions of the genome are isolated and sequenced. Targeted approaches allow researchers to reduce time and costs, and to limit data analysis on specific areas of interest.

Target genes can be captured in different ways, depending on the sequencing platform used. Among many current methods for targeted enrichment, the hybridization-based method is the most widely adopted (58).

Alternatively, it is possible to enrich target regions using PCR-base methods, e.g. with highly multiplexed PCR (59).

Both approaches present pros and cons, e.g. both probes and primers are designed based on information from gene annotation databases, thus unknown gene exons are typically not included in the designs, and regions containing a high GC percentage may hybridize or amplify poorly for enrichment. However, TRS allows sequencing specific subsets of genes with high accuracy (thanks to a deep achievable coverage), in a significantly shorter turnaround time, and with a more feasible and functionally interpretable data set for bioinformatic analysis.

The capacity to analyse thousands of genes simultaneously provides a powerful tool for detecting pathogenic mutations in disorders with genetic and phenotypic heterogeneity such as deafness, and for this reason many research laboratories developed custom TRS panel for the study of HHI/HHL (60, 61).

However, considering that 1% of human genes are thought to be necessary for normal hearing function (62), TRS approaches of known deafness-genes are not always conclusive.

In this light, WES has clearly proved to be a powerful tool for investigating the genetics of Mendelian disorders, such as NSHI/NSHL (63).

As for TRS, also WES enrichment methods may be based on hybridization or PCR techniques, with the same pros and limits.

Since the introduction of the first WES technology in 2004 (454 GS FLX (Roche)), more than 1000 NGS-related manuscripts have been published and approximately more than a quarter of all known NSHI/NSHL genes have been successfully determined in the last 5 years (63). Most likely, the identification of other deafness genes will soon follow.

This is an essential starting point for both uncovering the molecular mechanisms of HI/HL and for providing clues to therapeutic approaches.

2. AIMS OF THE STUDY

The definition of the molecular diagnosis of NSHI/NSHL is essential for both uncovering the molecular mechanisms of deafness, and for providing patients with prognostic information and personalized risk assessments.

Moreover, the achievement of a correct diagnosis contributes to reduce healthcare costs by directing the clinical evaluation and avoiding unnecessary tests such as the routine use of imaging.

The aim of this study is to define the genetic cause of hearing loss in a subset of NSHI/NSHL familial cases coming from both Italy and Qatar.

Considering the high genetic heterogeneity of this disease, and that different major players seem to be involved in the Italian and Qatari population (64), next generation sequencing techniques have been employed.

In particular, as a first step, patients have been screened for 96 deafness-genes using a custom targeted re-sequencing panel, in order to identify mutations in genes already known to cause NSHI/NSHL.

Where negative results were obtained with the first approach, families have been selected for whole exome sequencing analysis, with the purpose of discovering new genes involved in this disease.

Finding new NSHI/NSHL-causative genes will definitely increase our knowledge of the genetic basis and molecular mechanisms underlying this disorder, providing clues to new therapeutic options.

3. MATERIALS AND METHODS

3.1 Patients Selection and Recruitment

Subjects affected by NSHI/NSHL were recruited at ENT Department of IRCCS “Burlo Garofolo” in Trieste (Italy), ENT Department of IRCCS “Cà Granda Osp.Maggiore Policlinico” in Milan (Italy), ENT Department, Hamad Medical Corporation (HMC) in Doha (Qatar) and from other Genetics and ENT Clinics in Italy (in particular Torino, Siena, Ferrara, Monza, Cesena and Bologna).

A comprehensive family history was collected. In particular, for all Qatari families a special attention to consanguinity between parents has been paid.

A complete medical evaluation has been performed on each family to exclude hearing loss due to infections, trauma, or other non-genetic causes. Moreover, all family members underwent a fully medical ascertainment to exclude syndromic deafness.

All participants underwent pure tone audiometric testing (PTA) or auditory brainstem response (ABR) (depending on the probands' age) in order to characterise the severity of HI/HL according to the following guidelines (65):

- Slight: 16-25 decibels (dB)
- Mild: 26-40 dB
- Moderate: 41-55 dB
- Moderately severe: 56-70 dB
- Severe: 71-90 dB
- Profound: 91 dB or more

Based on the inheritance pattern, familial cases were further categorized as:

- a) Presumed autosomal recessive (consanguineous parents and/or affected siblings)
- b) Presumed autosomal dominant

All patients included in the study were negative for the presence of mutations in *GJB2* and *MTRNR1* genes.

A written informed consent was obtained from all participants; in case of minors, their next of kin provided written informed consent. The study was conducted in accordance with the tenets of the Helsinki Declaration and was approved by the Ethics Committee of IRCCS-Burlo Garofolo of Trieste (Italy) and the International Review Boards of Hamad Medical Corporation Doha (Qatar)

3.2 DNA Isolation and Quality Control

Genomic DNA was extracted from peripheral whole blood or saliva samples using a Qiasymphony instrument (Qiagen).

DNA quality was checked with a 1% agarose gel electrophoresis.

DNA concentration was measured with Nanodrop ND 1000 spectrophotometer (NanoDrop Technologies) and later verified with Qubit fluorometer (Thermo Fisher Scientific).

3.3 Targeted re-Sequencing (TRS)

3.3.1 Custom TRS Panel

A hearing loss TRS panel including known NSHI/NSHL genes, few NSHI/NSHL mimics, and some SHI/SHL genes was set up (66).

Genes' function was defined according to data obtained from scientific literature and from the most comprehensive public databases (Hereditary Hearing Loss Homepage, <http://hereditaryhearingloss.org>, Deafness Variation Database, <http://deafnessvariationdatabase.org/>, and Mouse Genome Informatics, <http://www.informatics.jax.org/>).

Briefly, 38 ARNSHI/ARNSHL genes, 20 ADNSHI/ADNSHL genes, 5 genes related to both dominant and recessive patterns of inheritance, 4 X-linked genes and 13 SHI/SHL genes were selected. Moreover 16 candidate genes have been included. These genes were selected based on the following criteria: genes related to hearing function and/or hearing loss in mice models, genes whose protein localization has been detected in ear structures, like cochlea or nervous hearing system, genes that are known to be involved in inner ear or hair cell development and cochlear wiring. The panel was designed using Ion AmpliSeq™ Designer v1.2 (Thermo Fisher Scientific).

Two primer pools (Pool 1: 1747 amplicons, Pool 2: 1740 amplicons) intended for DNA library construction through multiplex PCR were created. Targeted regions included coding regions (CCDS), 3' UTR, 5' UTR and 50 bp exon/intron boundaries of each of the 96 selected genes. The primer design ensures 92% overall targeted region coverage spanning through 411 Kbp.

All panel details are reported in **Table 3.1**.

AUTOSOMAL RECESSIVE GENES				
Gene	Loci	Covered Bases	Overall Coverage	Exons
<i>BDP1</i>	DFNB49	9389	85%	39
<i>CATSPER2</i>	DIS	2417	75%	15
<i>CDH23</i>	DFNB12	13861	95%	74
<i>CLDN14</i>	DFNB29	2274	97%	7
<i>COL11A2</i>	DFNB53/DFNA13	6561	97%	67
<i>DFNB59</i>	DFNB59	1481	97%	7
<i>ESPN</i>	DFNB36	3167	90%	13
<i>ESRRB</i>	DFNB35	2950	98%	11
<i>GIPC3</i>	DFNB15/DFNB95	3912	91%	6
<i>GJA1</i>	–	2898	93%	2
<i>GJB4</i>	–	2203	78%	2
<i>GPSM2</i>	DFNB32/82	2984	98%	15
<i>GRXCR1</i>	DFNB25	992	100%	4
<i>HGF</i>	DFNB39	4350	96%	21
<i>LHFPL5</i>	DFNB67	1612	75%	4
<i>LOXHD1</i>	DFNB77	8264	98%	47
<i>LRTOMT</i>	DFNB63	4187	76%	11
<i>MARVELD2/TRIC</i>	DFNB49	1789	83%	7
<i>MSRB3</i>	DFNB74	4101	88%	9
<i>MYO15A</i>	DFNB3	11057	93%	65
<i>MYO3A</i>	DFNB30	5741	99%	35
<i>OTOA</i>	DFNB22	2792	73%	30
<i>OTOF</i>	DFNB9	7755	99%	50
<i>PCDH15</i>	DFNB23/USH1F	12105	94%	43
<i>PDZD7</i>	–	4136	94%	18
<i>PTPRQ</i>	DFNB84	7000	93%	42
<i>RDX</i>	DFNB24	4128	92%	14
<i>SERPINB6</i>	DFNB91	1741	85%	8
<i>SLC26A4</i>	DFNB4	4035	82%	21
<i>SLC26A5</i>	DFNB61	2688	93%	21
<i>STRC</i>	DFNB16	1843	33%	29
<i>TMIE</i>	DFNB6	1852	100%	4
<i>TMPRSS3</i>	DFNB8/10	2289	82%	14
<i>TMPRSS5</i>	–	2165	98%	13
<i>TPRN</i>	DFNB79	2621	100%	4
<i>TRIOBP</i>	DFNB28	8861	82%	26
<i>USH1C</i>	DFNB18/USH1C	3320	100%	28
<i>WHRN</i>	DFNB31	4277	99%	14
Totals	38	169798	89%	840

AUTOSOMAL DOMINANT GENES				
Gene	Loci	Covered Bases	Overall Coverage	Exons
<i>ACTG1</i>	DFNA20/26	2039	91%	7
<i>CCDC50</i>	DFNA44	8092	90%	12
<i>CEACAM16</i>	DFNA4	1578	93%	7
<i>COCH</i>	DFNA9	2788	93%	13
<i>CRYM</i>	–	1488	93%	11
<i>DFNA5</i>	DFNA5	2495	97%	11
<i>DIAPH1</i>	DFNA1	5781	100%	28
<i>DIAPH3</i>	AUNA1	4832	96%	30
<i>DSPP</i>	DFNA39	2154	50%	5
<i>EYA4</i>	DFNA10	5533	96%	21
<i>GJB3</i>	DFNA28	3960	100%	4
<i>GRHL2</i>	DFNA28	5128	98%	16
<i>KCNQ4</i>	DFNA2	4089	100%	14
<i>MYH14</i>	DFNA4	6886	100%	43
<i>MYH9</i>	DFNA17	7505	100%	41
<i>MYO1A</i>	DFNA48	3613	100%	28
<i>POU4F3</i>	DFNA15	1182	100%	2
<i>SLC17A8</i>	DFNA25	2924	73%	12
<i>TJP2</i>	DFNA51	6867	97%	28
<i>WFS1</i>	DFNA6/14/38	3873	100%	9
Totals	20	82807	93%	342

AD/AR GENES				
Gene	Loci	Covered Bases	Overall Coverage	Exons
<i>GJB2</i>	DFNB1/DFNA3	2109	90%	2
<i>GJB6</i>		2399	96%	6
<i>MYO6</i>	DFNB37/DFNA22	7379	85%	35
<i>MYO7A</i>	DFNB2/DFNA11	8132	97%	53
<i>TECTA</i>	DFNB21/DFNA8/12	6457	100%	23
<i>TMC1</i>	DFNB7/11/DFNA36	2796	87%	24
Totals	5	29272	93%	143

X-LINKED GENES				
Gene	Loci	Covered Bases	Overall Coverage	Exons
<i>POU3F4</i>	DFNX2 (DFN3)	1165	77%	1
<i>PRPS1</i>	DFNX1 (DFN2)	2134	99%	7
<i>SMPX</i>	DFNX4 (DFN6)	934	100%	5
<i>TIMM8A</i>	DFN1	1882	94%	4
Totals	4	6115	93%	17

AR SYNDROMIC HL GENES				
Gene	Loci	Covered Bases	Overall Coverage	Exons
<i>ATP6V1B1</i>	–	1887	97%	14
<i>BCS1L</i>	–	1663	100%	9
<i>COL9A3</i>	–	2485	100%	32
<i>ERCC2</i>	–	3009	95%	25
<i>ERCC3</i>	–	2750	100%	15
<i>KCNE1</i>	–	2889	75%	6
<i>KCNJ10</i>	–	5306	100%	2
<i>LHX3</i>	–	2390	93%	7
<i>MTAP</i>	–	2969	60%	8
<i>SLC4A11</i>	–	3470	97%	22
Totals	10	28818	92%	140

AD SYNDROMIC HL GENES				
Gene	Loci	Covered Bases	Overall Coverage	Exons
<i>PAX3</i>	WS1/WS3	6147	100%	15
<i>PMP22</i>	–	3101	91%	8
<i>TCF21</i>	–	4155	93%	5
Totals	3	13403	95%	28

CANDIDATE GENES				
Gene	Loci	Covered Bases	Overall Coverage	Exons
<i>ACTB</i>	–	1763	97%	6
<i>AQP4</i>	–	5423	96%	6
<i>BSND</i>	–	1370	100%	4
<i>FGF3</i>	–	1543	100%	3
<i>GATA3</i>	–	3144	98%	7
<i>GJB1</i>	–	1733	100%	3
<i>GSTP1</i>	–	945	99%	7
<i>JAG1</i>	–	5820	97%	26
<i>MTAP</i>	–	2969	60%	8
<i>MYO1C</i>	–	4459	88%	34
<i>MYO1F</i>	–	4009	96%	28
<i>NR2F1</i>	–	1897	59%	3
<i>OTOR</i>	–	1463	99%	4
<i>SOX2</i>	–	2487	99%	1
<i>SPINK5</i>	–	3819	98%	35
<i>TBL1X</i>	–	5805	97%	20
Totals	16	48649	93%	195

GRAND TOTALS	
Number of genes included	96
Number of exons targeted	1,562
Number of BP covered	343,475
Mean overall coverage	92,4%

Table 3.1 Details of the custom targeted re-sequencing panel used in this study.

3.3.2 Library Preparation

DNA libraries were constructed using Ion AmpliSeq™ Library Kit 2.0 (Thermo Fisher Scientific).

Ten ng of genomic DNA were used. Target genes were amplified by highly multiplexed PCR according to the following protocol:

Component	Volume	Stage	Step	Temperature	Time
5X Ion AmpliSeq™ HiFi Mix	4 µl	Hold	Activate the enzyme	99°C	2 min
2X Ion AmpliSeq™ Primer Pool	10 µl	14 cycles	Denature	99°C	15 sec
DNA (10ng/6µl)	6 µl		Anneal and extend	60°C	8 min
Total	20 µl	Hold	-	10°C	Hold

Amplified DNA samples were then digested with 2 µl of FuPa enzyme (50°C for 10 min, 55°C for 10 min followed by the enzyme inactivation at 60°C for 20 min).

After digestion, DNA fragments were indexed using Ion Xpress™ Barcode Adapters 1-16 Kit (Thermo Fisher Scientific) adding 0,5 µl of Ion P1 adapter, 0,5 µl of Ion Xpress Barcode X, 1 µl of Nuclease free water, 4 µl of Switch solution and 2 µl of DNA Ligase (30 min at 22°C followed by ligase inactivation at 60°C for 20 min). Adaptor ligated amplicon libraries were purified with the Agencourt AMPure XP system (Beckman Coulter Genomics).

Libraries were quantified using KAPA Library Quantification Kits—Ion Torrent/Universal (KAPA Biosystems) and the 7900HT Fast Real Time PCR system (Applied Biosystems) and after diluted to 10pM.

Four indexed patients' libraries were pooled for one sequence reaction.

3.3.3 Template Preparation and Sequencing

Library fragments were amplified onto Ion Sphere™ particles by emulsion PCR using the Ion PGM™ Hi-Q™ OT2 Kit (Thermo Fisher Scientific) on the Ion OneTouch™ 2 instrument (Thermo Fisher Scientific).

After amplification the template-positive Ion Sphere™ particles were isolated using the Ion OneTouch™ ES (Thermo Fisher Scientific) and then loaded directly onto an Ion 318™ Chip (Thermo Fisher Scientific).

Fragments were sequenced using the Ion PGM™ Hi-Q sequencing kit (Thermo Fisher Scientific) on the Ion Torrent Personal Genome Machine (PGM) System (Thermo Fisher Scientific).

This platform uses the ion semiconductor technology, a method of sequencing by synthesis. The machine sequentially floods the chip with one nucleotide after another. The chip consists of ~11.3 millions of micro-wells that are associated to sensors able to detect pH change. If a nucleotide complements the sequence of the DNA molecule in a particular micro-well, it will be incorporated and hydrogen ions are released. The pH of the solution changes in that well and is detected by the ion sensor, essentially going directly from chemical information to digital information.

3.4 Whole Exome Sequencing (WES)

WES was performed at the Europe Life Technologies Ion AmpliSeq™ Exome Certified Service Providers, CRIBI Sequencing Core, University of Padua, Italy (67).

DNA libraries were prepared employing the Ion AmpliSeq™ Exome Kit (Thermo Fisher Scientific) and were then sequenced by the Ion Proton™ System (Thermo Fisher Scientific), according to standardized procedures.

Exome was enriched using a PCR-based method that targeted ~33 Mb of coding exons, thus greater than 97% of coding regions as described by Consensus Coding Sequences (CCDS) annotation. Twelve primer pools for highly specific enrichment of exons within the human genome were employed (total design coverage including padding and flanking regions is ~58 Mb).

3.5 Data Analysis

Both TRS and WES sequencing data were analysed with Ion Torrent Suite™ v4.0 software, set up with standardized parameters.

Single Nucleotides Variations (SNVs) and Small Insertions and Deletions (INDELs) were collected into a standardized Variant Call Format (VCF) version 4.1 (68). SNVs and INDELs were then annotated with ANNOVAR (69) using human genome build 19 (hg19) as the reference.

SNVs leading to synonymous amino acids substitutions not predicted as damaging and not affecting highly conserved residues were excluded, as well as SNVs/INDELs with quality score (QUAL) <20 and called in off-target regions.

A comparison between the identified genetic variants and data reported in NCBI dbSNP build137 (<http://www.ncbi.nlm.nih.gov/SNP/>) as well as in ExAC (<http://exac.broadinstitute.org/>), 1000 Genomes Project (<http://www.1000genomes.org/>) and NHLBI Exome Sequencing Project (ESP) Exome Variant Server (<http://evs.gs.washington.edu/EVS/>) led to the exclusion of those variants previously reported as polymorphism. In particular a Minor Allele Frequency (MAF) cut off of 0.01 and one of 0.001 were used for recessive and dominant families respectively.

The pathogenicity of known genetic variants was evaluated using ClinVar (<http://www.ncbi.nlm.nih.gov/clinvar/>), Deafness Variation Database (<http://deafnessvariationdatabase.org/>) as well as The Human Gene Mutation Database (<http://www.hgmd.cf.ac.uk/ac/index.php>).

On the other hand, for novel variants, several *in silico* tools, such as PolyPhen-2 (70), SIFT (71), MutationTaster (72), LRT (73), CADD score (74) were used. Moreover, the conservation of residues across species was evaluated by PhyloP (75) and GERP (76) scores.

Human Splicing Finder (HSF) version 2.4.1 (<http://www.umd.be/HSF/>) (77) and Splice Site Prediction by Neural Network (NNSPLICE) version 9 (www.fruitfly.org) were used to predict the effect of the mutations on splicing.

We manually investigated the raw sequence reads for all the candidate pathogenic variants using the Integrative Genomics Viewer (IGV) (78) with the purpose of excluding likely false positive calls due to read misalignment.

Finally, the most likely disease-causing SNVs/INDELs were analysed by direct Sanger sequencing on a 3500 Dx Genetic Analyzer (Applied Biosystems), using ABI PRISM 3.1 Big Dye terminator chemistry (Applied Biosystems).

Sanger sequencing was employed also to perform the segregation analysis within the family.

Moreover, an analysis of read depth in NGS data has been used to detect the presence of Copy Number Variations (CNVs).

To this aim, the sequence alignment data in BAM file format has been obtained from the Ion Torrent Suite™v4.0 and then analysed with CoNVaDING, a free tool recently developed to identify CNVs specifically from targeted NGS data (79). Briefly, for each patient the algorithm exploits the information of a set of control samples to detect any possible fall or increase in the patient's DNA that is not due by coverage noise but instead to the presence of DNA deletions or duplications.

The method consists of 4 steps:

1. Selection of control samples with a coverage pattern that is most similar to that of the sample analysed.
2. Normalization of coverage data across all samples in order to make it comparable.
3. Computation in each target of the ratio of the normalized average read depth of the sample to that of the controls and its examination for prediction of CNVs.

4. Analysis of the coverage of all the targets containing candidate CNVs and exclusion of those showing a high variability (indicating low-quality)

For each sample 30 control individuals were taken. The ratio cut-offs has been set as default (0.65, 1.4).

3.6 Functional Validation

In case of interesting results, functional experiments have been performed.

3.6.1 Protein Modelling

In order to test the effect of the most interesting mutations detected both in known deafness-genes and new candidates, protein modelling and molecular dynamics (MD) simulations were performed (in collaboration with Dr Navaneeth Krishnamoorthy, Sidra Medical Research Hospital-Qatar). In particular, the structural consequences of one missense mutation found in *CDH23* (UniProt: Q9H251), two missense mutations of *TMC1* (UniProt: Q8TDI8), and one nonsense, one frameshift and one missense mutation of *SPATC1L* (Uniprot ID: Q9H0A9) were further investigated. As regards *CDH23* and *TMC1*, for both regions investigated (cadherin domains 20-21 and *TMC1* residues 402-652 respectively), there were no 3D structures available. As a consequence, for *CDH23*, the crystal structure of mouse N-cadherin ectodomain protein (PDB ID: 3Q2W) (80), sharing 42% similarity with human *CDH23*, was used, while, for *TMC1*, the crystal structure of a calcium (Ca 2+) channel protein (PDB ID: 4WIS) from the fungus (*Nectria haematococca*)(81) that shares 26% similarity with human *TMC1* was considered. The quality of the models was evaluated using methods previously reported (82).

The constructed wild type structures were used for producing mutational models (p.P2205L in *CDH23* and p.R445H & p.L603H in *TMC1*) in the Discovery Studio (Accelrys Inc., San Diego, CA, USA) as described by Gajendrarao et al., 2013 (83) and

to identify functional (Ca²⁺ binding) sites and the key residues involved. PyMOL was used to visualize the proteins and to prepare model representations (www.pymol.org).

In the case of SPATC1L, since no homologues structures for modelling were available, a new structure, by applying iterative threading assembly refinement, was built (84). The quality of the wild type model was assessed by methods previously reported (82) that showed a biologically reliable model. To produce the mutants (Y282*, p.K115fs*12, p.Y219S), the wild type was used in the Discovery Studio (Accelrys Inc., San Diego, CA, USA) as described previously (83).

The wild type and mutant proteins were used in GROMACS simulation package for MD simulations by applying GROMOS96 force field (85–87). The proteins were solvated in the water model of SPC3 in a cubic box with a size of 1.5 nm (88). The systems were neutralized adding counter ions and the periodic boundary conditions were applied in all directions. The resulting systems contained from ~52000 to ~88000 atoms. For long-range interactions a twin range cut-off was used, i.e. 0.8 nm for van der Waals and 1.4 nm electrostatic interactions. The LINCS algorithm (89) was used to constrain all the bond lengths. To constrain the geometry of the water molecules, the SETTLE algorithm (90) was utilized. The systems were undergone to energy minimization using the steepest descent algorithm with the tolerance of 2000Kj/mol/nm followed by 100ps pre-equilibration and 10ns of production MD simulations. This is with a time-step of 2 fs at constant temperature (300 K), pressure (1 atm) and number of particles, without any position restraints (91). At every 100ps a structural snapshot was collected and the tools available within GROMACS were used for analysing the collected trajectories.

The cluster analysis was used to select the representative structures from MD simulations. Each simulation produced 10000 structures that were all grouped into clusters based on their structural deviation, in which the top ranked cluster was chosen for representation. The PyMOL package (www.pymol.org) was used for all

the graphical representations. Sequence alignment of human SPATC1L with mouse Speriolin (Uniprot: Q148B6) was performed using program CLUSTALO (<http://www.clustal.org/>).

3.6.2 *In vitro* Molecular Cloning

The impact of the identified mutations on mRNA and protein levels was tested by transient transfection in Hek 293 cells using expression clones containing either the wild-type (Wt) or the mutant cDNA. cDNAs were cloned into a pCMV6-Entry vector (Origene, Rockville, MD), Myc-tagged.

The calcium phosphate transfection method was used (92). Forty-eight hours after transfection total cell proteins and RNAs were prepared and analysed by Western blot and quantitative Real Time PCR (qRT-PCR), respectively.

3.6.2.1 Western Blot Analysis

For protein analysis, Hek 293 cells were lysed in IPLS buffer (50 mM Tris-HCL pH7.5, 120 mM NaCl, 0.5 mM EDTA and 0.5% Nonidet P-40) supplemented with proteases inhibitors (Roche). After sonication and pre-clearing, protein lysate concentration was determined by Bradford Assay (Biorad). An 8% polyacrylamide gel was used for protein electrophoresis. After blotting, membranes were blocked with 5% skim milk in Tris-buffered saline, 0.1% Tween 20 (TBST) and then incubated with primary anti-Myc antibodies overnight. Secondary antibodies were diluted in blocking buffer and incubated with the membranes for 45 min at room temperature. Proteins were detected with the ECL detection kit (GE Health Care Bio-Sciences).

Housekeeping proteins (e.g. β -actin or Hsp90) were used as an internal control for protein loading as well as for reference in the western blotting analysis.

3.6.2.2 Quantitative Real-Time PCR (qRT-PCR)

RNA was extracted from cell pellets using High Pure RNA isolation Kit (Roche). Total RNA (1 μ g) was reverse transcribed to cDNA using Transcriptor First Strand cDNA Synthesis kit (Roche). Quantitative Real time PCR (qRT-PCR) was performed using standard PCR conditions in a 7900HT Fast Real Time PCR System (Applied Biosystems) with Power SYBR Green PCR Master Mix (Thermo Fisher Scientific). Gene-specific primers were designed by using Primer3Web software (<http://bioinfo.ut.ee/primer3/>). All experiments have been performed in biological triplicate. Expression levels have been standardized to Neo gene expression and all data have been analyzed using the $2^{-\Delta\Delta CT}$ Livak Method (93).

3.6.3 *In vivo* expression studies

Expression studies in mouse tissues or in Zebrafish larvae have been performed to test the expression profile of different genes of interest.

3.6.3.1. Gene expression in mouse tissues

Total RNA samples were extracted from wild-type CD1 mouse whole cochleae at post-natal day 3 (P3), P8, P12 and 2 month-old. Moreover, total RNA from different tissues, including liver, spleen, lung, kidney, brain, testis and heart, was extracted from 2-month old mice. The extraction was made using Direct-zol RNA MiniPrep Kit (Zymo Research). RNA was quantified using Nanodrop ND-1000 spectrophotometer (NanoDrop Technologies). Complementary DNAs were generated from 1 μ g of total RNA using the Transcriptor First Strand cDNA Synthesis Kit (Roche) according to the manufacturer's protocol. cDNAs were used for semi-quantitative RT-PCR (sqRT-PCR) or quantitative RT-PCR (qRT-PCR). In the case of sqRT-PCR, 6 μ l of the RT products was used for PCR amplification, while for qRT-PCR 2 μ l of the RT products was used for Real Time PCR. Gene-specific primers were designed by using Primer3Web

software (<http://bioinfo.ut.ee/primer3/>). sqRT-PCR amplified products were resolved on 2% agarose gels and visualized by EB staining.

qRT-PCR expression levels have been standardized to β Actin gene expression and all data were analyzed using the $2^{-\Delta\Delta CT}$ Livak Method (93).

The experiments were performed in biological triplicates. β Actin primers were used as internal control.

3.6.3.2. Gene expression in Zebrafish larvae

Gene expression in Zebrafish larvae (5 days post fertilization (dpf)) was performed in collaboration with ZeClinics (Barcelona, Spain).

Whole mount in situ hybridization (ISH) was carried out.

Specific riboprobes intended to recognize the mRNA of the genes of interest were designed. cDNAs were amplified by PCR from a custom Zebrafish cDNAs library obtained by RT-PCR from a mRNA pool coming from 5 dpf Zebrafish larvae. A T7 sequence linker in reverse primers was included to directly use the synthesized PCR products as templates to amplify the reverse digoxigenin-labeled riboprobe to be used for ISH.

Once dissected, embryos were fixed in 4% paraformaldehyde (PFA) over night, and then dehydrate with increasing concentrations of Metanol PBT for long-term storage. Embryos were then rehydrated, dechorionated and treated with proteinase K. Afterwards embryos were incubated with a hybridization mix containing the riboprobe and then with antibody against digoxigenin. Nitroblue Tetrazolium (NBT) was used with the alkaline phosphatase substrate 5-Bromo- 4-Chloro-3-Indolyl Phosphate (BCIP). These substrate systems produce an insoluble NBT diformazan product that is blue to purple in color and can be observed visually (94).

In order to check gene expression in hair cells, marked with GFP through its activation by the Brn3c promoter, secondary antibody against GFP was used.

Stained embryos were processed for imaging through 2 different methods:

1. Whole embryos were imaged with a bright field stereoscope to determine the overall expression pattern.
2. Transversal sections were acquired through a cryostat (20 μm width) to determine precisely the mRNA location within the inner ear across 3 different anteroposterior positions. Gene expression pattern was compared with the position of hair cells, marked with GFP through its activation by the Brn3c promoter. Sections were imaged with Leica DM5 light/fluorescent microscope at 40x magnification.

4. RESULTS AND DISCUSSION

4.1 Patients

A total of 32 Italian and 27 Qatari probands affected by NSHL and their relatives (when available) for a grand total of 305 samples, were sequentially collected during the past three years.

Based on the family history, Italian cases were categorized as presumed autosomal recessive (15%), presumed autosomal dominant (78%) and ambiguous (7%), while all Qatari cases were categorized as presumed autosomal recessive (100%).

The most common characteristics of our probands included:

- pediatric age (60% were < 18 years)
- childhood hearing loss (48%)
- severe-profound hearing loss (51%)

4.2 Targeted Resequencing (TRS)

TRS, based on Ion Torrent PGMTM technology was applied to 32 Italian families and 18 Qatari families, negative for mutations in *GJB2* and for the A1555G mitochondrial mutation.

On average 95% of the targeted region was covered at least 20X, and 334,12 mean-depth total coverage was obtained. A total of 170 Mbp of raw sequence data was produced per individual.

We identified an average of 503,2 genetic variants (SNVs/INDELs) per subject, and after the filtering pipeline described in the Materials and Methods section an average of 17 residual SNVs/INDELs for each subject remained.

After segregation analysis, a molecular cause was identified in 16 Italian and 9 Qatari families, for an overall detection rate of 50% (**Table 4.1**)

ID	Origin	Inheritance Pattern	Affected members	Type of HL	Gene	Variant	Zygosity	Frquency (ExAc)	Path Pred ¹	Reference
Family_1	Italy	AR	2 siblings	Postlingual bilateral asymmetric moderate to severe high frequencies SNHL	<i>TMPRSS3</i>	NM_024022.2 :c.C1019G:p.T340R;	het	NA	4/4	This study
					<i>TMPRSS3</i>	NM_024022.2:c.C1291T:p.P431S	het	2,48E-05	4/4	(Vozzi et al., 2014)(66)
Family_2	Italy	AD	2 siblings, F, U, PGM	Postlingual bilateral symmetric moderatly-severe SNHL	<i>TECTA</i>	NM_005422:c.G775C:p.G259R	het	NA	4/4	This study
Family_3a ²	Italy	AD	2 siblings, F, U, and other relatives	Adult onset progressive moderate high frequencies SNHL	<i>DFNA5</i>	NM_001127454:c.666_669delCTAC:p.Y223Sfs*49	het	NA	1/1	This study
Family 3b ²				Childhood onset moderate SNHL	<i>GJB2</i>	NM_004004:c.G109A:p.V37I	het	6,59E-03	3/4	(Abe et al., 2000) (95)
					<i>GJB2</i>	NM_004004:c.T101C:p.M34T	het	8,50E-03	3/4	(Kelsell et al., 1997) (96)
Family_4	Italy	AR	2 siblings	Prelingual bilateral moderate symmetric SNHL	<i>STRC</i>	Whole gene deletion	hom	NA	NA	(Vona et al., 2015) (97)
Family_5	Italy	AD	2 siblings, F, PGM	Postlingual bilateral symmetric severe to profound progressive SNHL	<i>MYO6</i>	NM_004999:c.A599G:p.N200S	het	NA	3/3	This study
Family_6	Italy	AD	2 siblings	Adult onset bilateral mild-moderate symmetric SNHL	<i>ACTG1</i>	NM_001199954:c.A847G:p.M283V	het	NA	3/4	This study
Family_7		AD	P, F, U, PGM and other relatives	Postlingual bilateral symmetric moderate to severe progressive SNHL	<i>POU4F3</i>	NM_002700:c.G690C:p.R230S	het	8,28E-06	4/4	This study
Family_8	Italy	AR	2 siblings	Postlingual bilateral symmetric moderate to severe SNHL	<i>MYO7A</i>	NM_000260:c.G1556A:p.G519D	het	1,67E-05	4/4	(Bharadwaj et al., 2000) (98)
					<i>MYO7A</i>	NM_000260:c.G3670A:p.A1224T	het	4,37E-05	4/4	This study
Family_9	Italy	AD	P, M	Postlingual bilateral symmetric mild to moderate progressive SNHL	<i>MYH14</i>	NM_001145809:c.G1150T:p.G384C	het	2,86E-03	2/2	(Donaudy et al., 2004) (99)
Family_10	Italy	AD	P, M	Postlingual bilateral symmetric moderate to severe SNHL	<i>MYO7A</i>	NM_000260.3:c.C4268T:p.T1423M	het	3,64E-05	3/4	This study

Family_11	Italy	AD	P, F, A, PGF	Congenital bilateral mild to moderate symmetric SNHL	<i>TECTA</i>	NM_005422:c.G589A:p.D197N	het	NA	4/4	(Hildebrand et al., 2011)(100)
Family_12	Italy	AR	P, F, U, PGM	Postlingual bilateral symmetric moderate SNHL	<i>KCNQ4</i>	NM_172163:c.G947T:p.G316V	het	NA	4/4	This study ³
					<i>KCNQ4</i>	NM_172163:c.A1438G:p.I480V	het	NA	3/4	This study ³
Family_13	Italy	AD	3 siblings, F	Congenital bilateral severe symmetric SNHL/ severe high frequency SNHL	<i>TECTA</i>	NM_005422:c.6000-1G>T	het	NA	1/1	This study
Family_14	Italy	No FH	P	Congenital bilateral mild to moderate symmetric SNHL	<i>PDZD7</i>	NM_001195263:c.G329A:p.G110D	hom	NA	4/4	This study
Family_15	Italy	No FH	P	Postlingual bilateral symmetric moderate to severe SNHL	<i>POU3F4</i>	NM_000307:c.G989A:p.R330K	hem	NA	3/4	This study
Family_16	Italy	No FH	P	Postlingual bilateral symmetric moderate SNHL	<i>SLC26A4</i>	NM_000441:c.T1790C:p.L597S	hom	8,26E-03	4/4	(Yuan et al., 2012) (101)
Family_17	Qatar	AR	P	Pre-lingual bilateral severe to profound SNHL	<i>CDH23</i>	NM_022124:c.C6614T:p.P2205L	hom	NA	4/4	This study
Family_18	Qatar	AR	P							
Family_19	Qatar	AR	3 siblings							
Family_20	Qatar	AR	P	prelingual bilateral profound SNHL	<i>GJB6</i>	NM_006783:c.C209T:p.P70L	hom	1,65E-05	4/4	This study
Family_21	Qatar	AR	2 siblings	prelingual profound NSHL early onset profound NSHL	<i>TMC1</i>	NM_138691:c.G1334A:p.R445H	hom	8,24E-06	4/4	(Kalay et al.,2005) (102)
Family_22	Qatar	AR	P			NM_138691:c.1808T>A:p.L603H	hom	NA	4/4	This study
Family_23	Qatar	AR	2 siblings	early onset severe to profound NSHL	<i>MYO6</i>	NM_001300899:c.G178C:p.E60Q	hom	6,06E-05	4/4	This study
Family_24	Qatar	AR	P	early onset bilateral severe NSHL	<i>OTOF</i>	NM_194322:c.G169T:p.E75X	hom	NA	2/2	(Rodríguez-Ballesteros et al. 2008) (103)
Family_25	Qatar	AR	3 siblings,	congenital severe NSHL	<i>OTOA</i>	all gene deletion	hom	NA	NA	(Shahin H et al.,

Table 4.2 Causative mutations. In bold are the novel mutations. ¹ Prediction consensus value indicates the number of prediction scores which reports if the variant is likely to be disease causing or conserved. The following scores vote in towards consensus: SIFT (≤ 0.05 "D"), LRT ("D"), Mutation Taster ("A" or "D"), polyPhen2 HDIV ("P" or "D"). ² Family_3 is a multigenerational family in which we detect two different causative genes segregating in the same pedigree. ³ Both *KCNQ4* variants co-segregate in the affected members of this AD family. Legend: P= Proband, F= Father, M= Mother, U= Uncle, A= Aunt, PGM= Paternal Grand Mother, PGF= Paternal Grand Father.

We found that 82% of variants were missense, one was a frameshift deletion, one a splice-site variant, one a stop-gain mutation and 2 were large deletions.

Among the identified mutations, 13 were novel. In particular, in the Italian population new mutations in *TMPRSS3*, *DFNA5*, *MYO6*, *ACTG1*, *TECTA*, *PDZD7*, *KCNQ4* and *POU3F4* genes were identified, while in the Qatari population new variants in *CDH23*, *MYO6* and *TMC1* were discovered.

Consistent with literature data (105) our results confirmed that different genetic players are involved in the Italian population compared with the Qatari one, and that, even though the number of Qatari families analysed is lower, the Italian population seems to be characterised by a higher genetic heterogeneity, both in terms of genes and mutations (**Figure 4.1**).

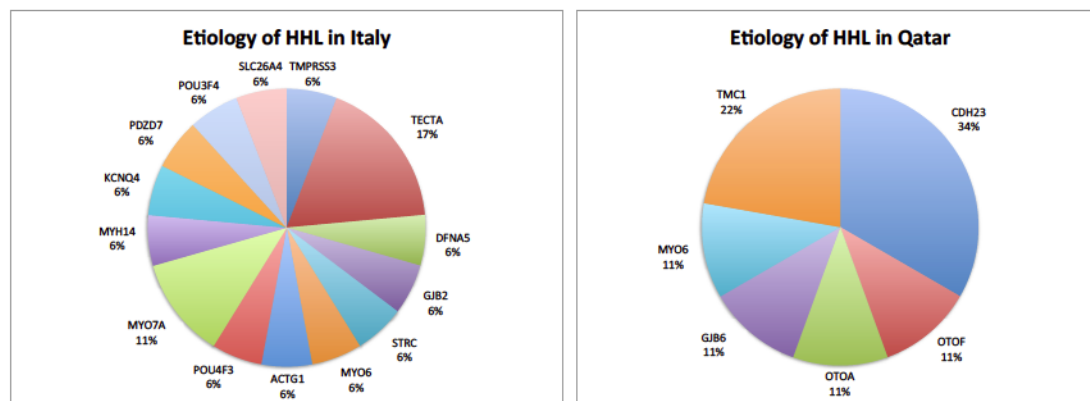


Figure 4.1 Distribution of causative HHL genes in our populations. As expected different genetic players are involved in the etiopathogenesis of HHI/HHL in the Italian and Qatari populations. Moreover, a higher genetic heterogeneity characterized the Italian families compared to the Qatari ones.

In our cohort of Italian families two genes were more frequently mutated: *TECTA* and *MYO7A*.

As regards *TECTA*, which encodes the α -tectorin, a non-collagenous proteins of the tectorial membrane, three different alleles have been identified in 3 families presenting an early onset, symmetrical ADNSHL, with different degrees of severity.

One of these mutations (NM_005422:c.G589A:p.D197N) was already known for causing NSHL (100), while the other two (NM_005422:c.G775C:p.G259R; NM_005422:c.6000-1G>T) were identified in the present study.

All the mutations affect functional domains of the α -tectorin (the entactin (ENT)-like, zonadhesin (ZA), and zona pellucida (ZP) domains respectively), involve highly conserved residues, and are predicted as pathogenic.

Even though with different alleles, *TECTA* represents one major player in our Italian population, suggesting that DFNA8/12 is one of the most frequent subtypes of autosomal dominant hearing loss.

As concerns *MYO7A*, which encodes the unconventional myosin7A, we identified three different alleles affecting two families of our cohort.

Mutations of this gene have been associated to Usher syndrome type 1b, ARNSHL and autosomal dominant NSHL (ADNSHL) (12).

Thanks to our TRS panel we identified two heterozygous missense mutations in one family with two affected siblings (compound heterozygotes) and healthy parents (carriers): the first (NM_000260:c.G1556A:p.G519D) described as causative of Usher 1b (98), and the second (NM_000260:c.G3670A:p.A1224T) described in the ExAC database with a very low frequency (MAF:4.371e-05). Interestingly this second variant interests the same amino acidic residue described by Ma et al. (106) (who reported the p.A1224D mutation) as associated to Usher syndrome 1b. In this light, despite patients showed only moderate to severe sensorineural HL, considering their young age (5 and 10 y.o.) and the fact that Usher syndrome 1b is characterised by adolescent-onset retinitis pigmentosa (107), it is highly recommended to perform some routine ophthalmologic tests.

This result highlights how genetic tests may lead to a proper diagnosis even before the appearance of clinical symptoms, thus correctly guiding the clinical management of patients.

In the second family, affected by ADNSHL, a heterozygous missense mutation was identified. The mutation (NM_000260:c.C4268T:p.T1423M), described in the ExAC database with a very low frequency (MAF: 3.636e-05), and predicted as damaging, affects a functional domain of the protein, the B41 domain, which is a plasma membrane binding domain. The substitution of a polar hydrophilic Threonine with a non-polar hydrophobic Methionine may alter protein structure, leading to clinical consequences. Interestingly the proband presents a phenotype very similar to the one described in another ADNSHL case due to a *MYO7A* mutation (108).

In the Qatari population, two genes, *CDH23* and *TMC1*, showed a higher prevalence, being mutated in three and two families respectively.

As regards *CDH23*, which encodes the cadherin 23 protein, we identified a homozygous missense mutation (NM_022124:c.C6614T:p.P2205L) never described in the ExAC database or associated with hearing phenotype in three consanguineous families affected by ARNSHL. Until now 14 *CDH23* missense mutations were reported in affected families of Middle Eastern populations (Jewish-Algerian, Palestinian, Turkish, Iranian and Pakistani (104, 109–112)). Interestingly, among them the p.D2202N variant is located in the same protein domain of the mutation identified in this study (110–112). Considering that the c.C6614T allele affects 17% of our cohort of families a molecular protein modelling, in collaboration with Dr. Navaneeth Krishnamoorthy (Sidra Medical Research Hospital-Qatar) was performed.

The protein modelling analysis revealed the relation between p.D2202 and p.P2205 residues as they both share the same structural loop that is directly involved in the formation of the functional Ca^{2+} binding site. In the case of p.P2205L mutation, the change from a Proline (cyclic structured side chain) to a Leucine (linear structured side chain) impacts the loop structure and the negatively charged Ca^{2+} binding site, and thereby the regular function of the protein (**Figure 4.2**).

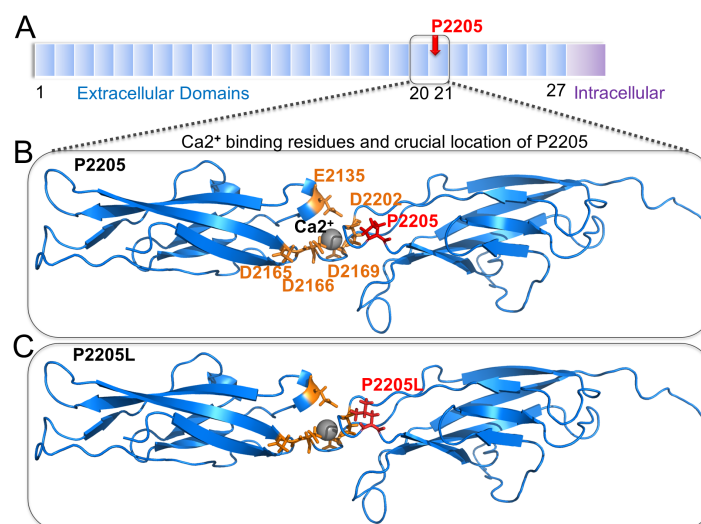


Figure 4.2. Molecular models of CDH23 protein. (A) Schematic diagram of CDH23 where the red arrow indicates the mutational region. (B) The 3D model structures of (B) p.P2205 and (C) p.P2205L of CDH23. Here, the functional site residues are in orange sticks around the Ca^{2+} as a gray sphere.

The other gene found mutated in two different families is *TMC1*, which encodes the Transmembrane Channel Like 1 protein. We identified two homozygous missense mutations affecting patients presenting an early onset profound NSHL.

The first one (NM_138691:c.G1334A:p.R445H) was previously reported in Turkish, Pakistani and Chinese families (102, 113, 114), while the second one (NM_138691:c.T1808TA:p.L603H), is a novel variant, located in a highly conserved region of the protein. Recently Bakhchane et al. described a missense variant located only one amino acid after the p.L603 residue that was classified as pathogenic after a 3D modelling approach (115).

With the finding of these two mutations, this gene seems to play a significant role in the Qatari population, affecting 11% of our families. In this light we decided to perform a protein modelling of both mutations, in collaboration with Dr. Navaneeth Krishnamoorthy (Sidra Medical Research Hospital-Qatar), in order to further prove their pathogenic role.

The modelled structure confirmed the pathogenic role the first allele (**Figure 4.3**).

For the second mutation (p.L603H), our molecular modelling correlates with the computational structure previously described by Bakhchane et. al (Figure 4.3). In particular, the substitution of a hydrophobic Leucine with a positive charged Histidine can impact the local structural integrity.

Overall, we can hypothesize that the replacement of residues with long (R) and short (L) linear side chains at 445 and 603 positions with an Histidine that has an imidazole ring as a side chain most likely alters the normal protein function (**Figure 4.3C**). Altogether, these mutations could introduce structural destabilization on both the sides to affect the nearby Ca²⁺ binding residues (p.N576, p.A579 and p.S608) thus leading to malfunction of TMC1.

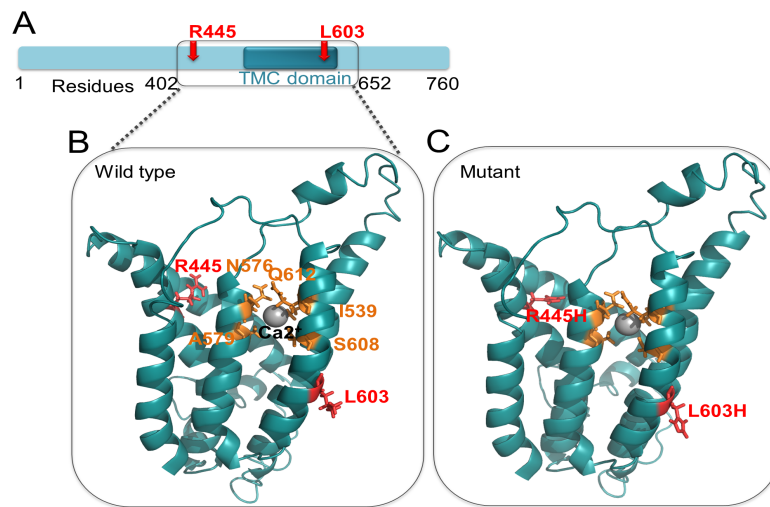


Figure 4.3. Molecular models of TMC1 protein. (A) Schematic representation of TMC1, where the red arrows show the location of the mutations. Molecular models of (B) wild type and (C) mutant of TMC1. Here, the functional site residues are in orange sticks around the Ca²⁺ as a gray sphere.

Interestingly both in the Italian and in the Qatari populations we were able to identify two CNVs affecting *STRC* and *OTOA* genes respectively.

CNVs have recently been found to be an important cause of NSHL (116). The main example is the deletion of the region of chromosome 15 that includes the *STRC* gene and that can cause ARNSHL (117) or deafness-infertility syndrome (DIS) in males if the adjacent *CATSPER2* gene is also involved in the deletion (118). *STRC* deletions frequency have been calculated to be of >1% in mixed deafness populations (119, 120) making it a major contributor to congenital hearing impairment. In our study we identified a homozygous deletion (chr15:43,891,024-43,940,259) of 49 Kb, spanning the whole *STRC* gene and *CATSPER2* gene in an Italian NSHL family characterized by an autosomal recessive pattern of inheritance. The family consists of 4 members, 2 affected siblings (a 5-year-old girl and a 3-year-old boy) and their normal hearing parents. Both children showed a bilateral moderate symmetric SNHL characterized by a pre-lingual onset. Considering that the deletion involved also *CATSPER2* gene it would be important to evaluate any fertility problems in the male proband.

The second most common CNV described in NSHL involves *OTOA* gene. In particular Shahin H et al. identified a large genomic deletion (500kb size) spanning *OTOA* harboured by a family of Arabic origin (Palestine), and estimated a carrier frequency of 1% in unrelated

Palestinian controls (104). In this study, we found a large homozygous deletion in three affected children of a Qatari consanguineous family, with healthy parents. The deletion spans through at least 58.016 bp (chr16:21,689,514-21,747,721), encompassing almost most of the *OTOA* genomic region (chr16:21,678,514-21,760,729) and it is included in that previously reported by Shahin H et al. This finding suggests that *OTOA* deletions should be further investigated in Arabic populations, and thus included in routine screening. Overall these results confirmed the importance of CNVs analysis in NSHL patients.

4.3 Whole Exome Sequencing (WES)

Eleven Italian and three Qatari families, that have been shown to be negative for TRS, have been selected for WES analysis (using the Ion Proton™ platform-LifeTechnologies).

Families were selected based on the following criteria:

1. Well-defined phenotype and consistent between the affected members of the pedigree;
2. Multigenerational pedigree with affected subjects in different generations;
3. Availability of complete clinical information, in particular audiometric information;
4. Availability of DNA samples of at least 4 family members (both affected and non affected).

So far, WES analysis led to the identification of two new HL-candidate genes: *SPATC1L* and *PLS1* in two ADNSHL Italian families.

The remaining 11 families are now going through data analysis and variants filtering steps.

4.3.1 *SPATC1L*

In this study, an Italian ADNSHL family (**Figure 4.4A**) showing a moderately severe to profound progressive hearing impairment (**Figure 4.4B**) was analysed by WES.

In particular subjects I:1, II:1, II:2, II:3, II:4 and III:1 were selected for the sequencing.

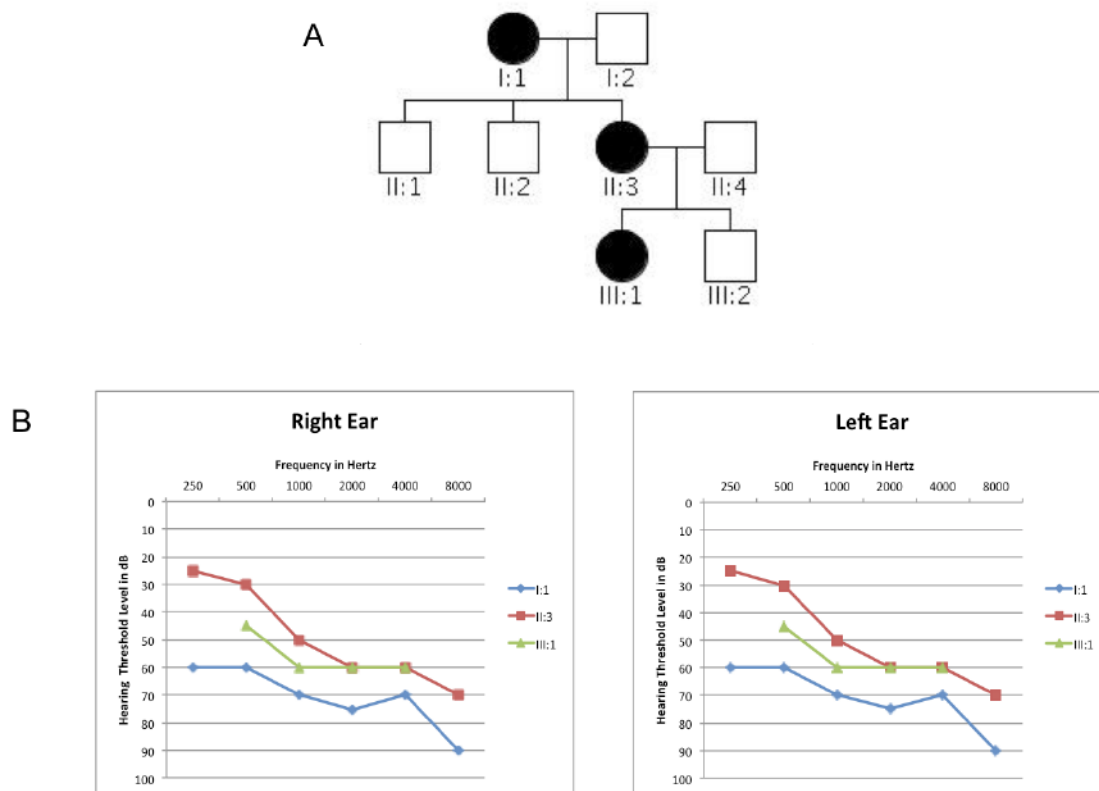


Figure 4.4. Pedigree and clinical features of the family. (A) Pedigree of the Italian family carrying the mutation in *SPATC1L* gene. Filled symbols represent affected individuals. (B) Audiograms of the patients (I:1, II:3, III:1, II:4).

The overall mean-depth base coverage for WES was 108X, while on average 89% of the targeted region was covered at least 20-fold. A total of 91.597 genetic variants were called among the six subjects included in WES study. After variants-filtering procedure, we identified 8 candidate single nucleotide variants (SNVs). Three of them were excluded because of their recurrence in our internal sequencing database (i.e. NGS data from overall 1071 unrelated individuals). The remaining ones have been prioritized according to: 1) role of the gene based on literature research, 2) type of mutation. Four missense mutations affecting genes associated to specific syndromes i.e. *COL11A1* associated to Stickler Syndrome (OMIM 604841), Marshall Syndrome (OMIM 604841) and Fibrochondrogenesis 1 (OMIM 228520), *GUCY2C* associated to Meconium Ileus (OMIM 614665) and Diarrhea (OMIM 614616), or phenotypes clearly not present in any of the affected members, i.e. *ZNF236* associated to congenital aural atresia in 18q deletion syndrome (121), *FSTL5* possibly involved in maintaining odor perception in mouse (122) and described as a tumoral

biomarker (123), were excluded from the analysis. The remaining nonsense mutation, c.C846G (NM_001142854, ENST00000291672.5), was present in *SPATC1L* gene and leads to a premature stop codon with the loss of the last 58 amino acids of the protein (p.Y282*). This mutation causes the loss of a series of highly conserved residues (Figure 4.5B), and was not described in any public database or in our internal database. Sanger sequencing demonstrated the correct segregation within the family (Figure 4.5A).

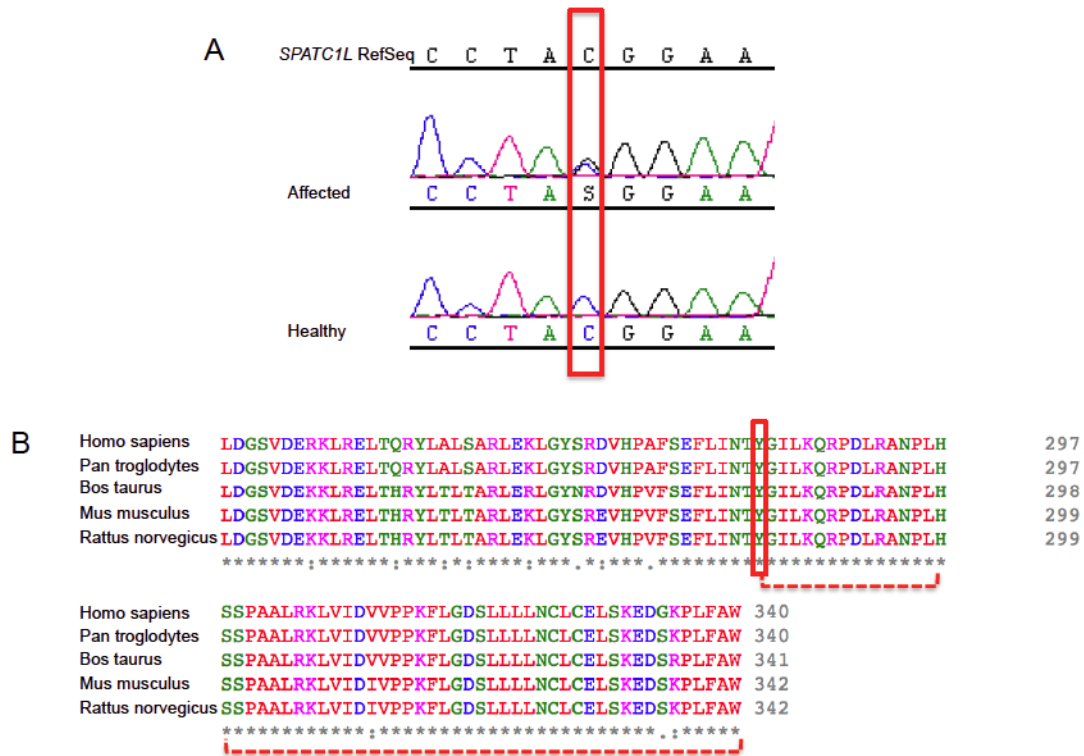


Figure 4.5 DNA sequence chromatograms and protein sequence alignment. (A) The figure displays DNA sequence chromatograms showing the nucleotide variant identified in *SPATC1L*. (B) Protein alignment shows conservation of the mutated residue across species. Dashed lines indicate the series of amino-acids lost.

Interestingly two independent analyses conducted in our laboratory supported the possible involvement of this gene in the auditory function/loss. In particular, a candidate-gene population-based statistical study in cohorts from Caucasus and Central Asia revealed a significant association of this gene with normal hearing function at low and medium hearing frequencies, and TRS of a cohort of 464 age-related hearing loss (ARHL) patients led to the identification of two deleterious *SPATC1L* mutations.

More in details, as regards the candidate-gene population-based statistical study, 604 people from several rural communities located along the Silk Road countries were collected (124). Audiometric tests and a clinical examination were carried out for each individual. From the six hearing thresholds values collected, three pure tone averages (PTAs) of air-conduction thresholds were calculated: PTAL at low frequencies (0.25, 0.5 and 1 kHz), PTAM at middle frequencies (0.5, 1 and 2 kHz) and PTAH at high frequencies (4 and 8 kHz). These three PTAs were used as quantitative traits in the association analysis. Moreover, to avoid non-genetic variations in the hearing phenotype (e.g. monolateral hearing loss), the best hearing ear was considered for the analyses. Subjects affected by syndromic forms or other systemic illnesses linked with sensorineural hearing loss were excluded. DNA samples were genotyped with the Illumina Exome Chip and a candidate gene association study was performed for three different traits (PTAs) on common variants only (MAF>0.01). A linear mixed model was applied with sex and age as covariates and the kinship matrix as the random effect in order to account for population structure and relatedness. Statistically significant associations were obtained for PTAL and PTAM with 3 *SPATC1L* coding SNPs (rs14378, rs113710653 and rs113146399). The most associated SNP was rs113710653 ($p=0.00564$). People carrying the alternative allele have worse hearing, taking into account sex and age differences. In particular, homozygote TT subjects show at PTAL and PTAM an increased dB threshold (+2.3 dB and 3.27 on average respectively) compared to the wild type (CC) ones (OR=1.17, 95% CI=[1.05-1.31] for PTAL and OR=1.20, 95% CI=[1.05-1.38] for PTAM).

Simultaneously TRS of 464 ARHL patients revealed the presence in *SPATC1L* of one frameshift (c.343_344insTTCA:p.K115fs*12) and one missense mutation (c.A656C:p.Y219S) in two unrelated patients. The frameshift variant was detected in a patient (Arhl_1) coming from Carlantino (an isolated village from Southern Italy). In this case, the availability of extended pedigrees and samples from the whole village population allowed us to look for segregation of this allele in other family members. Despite we are dealing with a late onset disease where frequently there are no other alive family members, we were able to exclude the presence of this allele in the only alive and aged relative of Arhl_1 (i.e. a healthy first cousin aged 68 years old). The c.A656C:p.Y219S variant was detected in a patient (Arhl_2) from Milan (Italy). All *in silico* predictor tools classified this allele as damaging. Both alleles

were confirmed by Sanger sequencing and were the only ultra rare (i.e. not described in any public database) and pathogenic variants present in Arhl_1 and Arhl_2 cases.

Unfortunately little is known about the role of *SPATC1L* gene. It encodes two different isoforms of the Speriolin-Like Protein, derived from alternatively spliced mRNAs, whose function is still unknown. A study from Lecat et al. 2015, revealed that SPATC1L protein localises in the cytoplasm, in the nucleus and in the perinuclear region in Hek293 cells, and after activation of the NK2 receptor it moves to cellular junctions, suggesting a possible role of this protein in cell junction formations (125). One major type of cells junctions are gap junctions which exist extensively in many different part of the cochlea and that have many hypothetical functions in this organ, such as K⁺ recycling, endocochlear potential generation, intercellular signalling, nutrient and energy supply etc. (126). To date, apart from the role of Connexins family and few others proteins (i.e. Pannexins family) (127), little is known about functions of other proteins in cell junctions. Considering the importance of these cellular components in hearing function, the role of SPATC1L and other related proteins needs to be further investigated.

It has also been shown that *SPATC1L* modulates the response of human cells to alkylating agents, having a protective effect. As a matter of facts, a decreased gene expression correlates with an increased sensitivity to alkylating agents, such as N-methyl-N'-nitro-N-nitrosoguanidine (MNNG) (128). Further investigations on how *SPATC1L* plays this role will help in understanding if it is involved in processes that guarantee cell survival in response to damaging agents or oxidative stress, a major cause of ARHL and hearing dysfunction. Accordingly, some ARHL candidate genes so far described are involved in oxidative stress response and mitochondrial dysfunction (129).

In order to better characterise the role of this gene and the effect of the identified mutations, some functional experiments have been performed.

First of all, the impact of all mutations was analysed by molecular dynamics (MD) simulations.

As expected, the wild type system showed a stable behaviour by maintaining secondary structures (**Figure 4.6D-G**), as opposed to all mutants. In particular, MD of the SPATC1L systems demonstrated:

a) A reduced structural stability for the p.Y282* mutant in addition to the loss of part of the C-terminal (283-340) and mild alteration of the secondary structures at the N-terminal.

b) A reduced structural stability for the p.K115fs*12 mutant plus the loss of ~75% of the protein (126-340) including the C-terminal and a decreased stability leading to a disordered protein isoform.

c) An increased structural stability and rigidity for the p.Y219S mutant and no loss of secondary structures.

It is interesting to notice that all variants affect the C-terminal of SPATC1L that seems to contain important functional domains. In fact sequences alignment of human SPATC1L and mouse SPATC1 (encoded by *Spatc1*, the orthologous gene of the human *SPATC1*, a paralog of *SPATC1L*) revealed that most of the conserved regions of mouse SPATC1, which correspond to the N- and C-terminals, are conserved also in human SPATC1L. In particular, the C-terminal contains the binding region for cell-division cycle protein 20 (Cdc20) that according to sequence similarity is most likely present also in the human SPATC1L (**Figure 4.6A-B**).

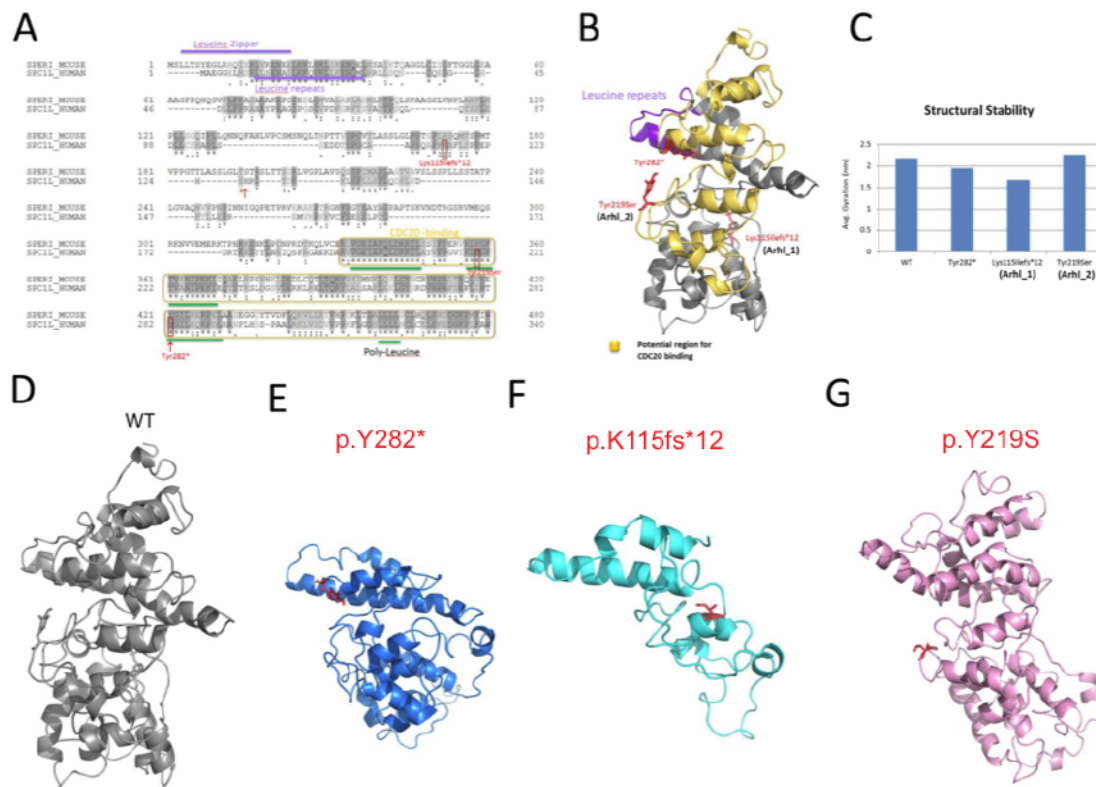


Figure 4.6 Sequence analysis and molecular modelling of the proteins. (A) Sequence alignment of human Speriolin-like protein (Q9H0A9) with mouse Speriolin (Q148B6). (B) Molecular model of the human SPATC1L with potential functional regions. (C) Average radius of gyration of the four systems. (D-G) Representative

structures of the WT, Y282*, p.K115fs*12 and p.Y219S, from molecular dynamics simulations. Here, the locations of the mutations are represented as red sticks.

Overall these findings suggest that all mutations lead to new isoforms with reduced or/and increased structural stability, which may generate partial or non-functional proteins, or to proteins with inadequate flexibility (that is normally required for the correct functionality). Afterwards the effect on mRNA and protein levels of all the *SPATC1L* mutations identified in this study was tested *in vitro*, using expression vectors containing either the Wt or the mutant cDNAs.

In particular, qRT-PCR didn't reveal any significant difference in the expression levels of all mutants compared to the Wt (**Figure 4.7A**).

WB analysis confirmed the presence of all mutated protein isoforms (**Figure 4.7B**). In the case of the missense mutation of Arhl_2 patient (p.Y219S), a full-length protein was detected. On the contrary, in the case of the two truncating variants carried by Arhl_1 patient and by the Italian family (p.K115fs*12 and p.Y282* respectively), shorter protein isoforms were observed. Interestingly, in the case of the frameshift insertion (patient Arhl_1), two different bands were detected: a higher one, with the expected molecular weight, and a smaller one. Considering the huge impact of this mutation on protein structure, it is highly probable that the truncated isoform will be rapidly degraded, thus the shorter band in the WB may represent a pattern of protein degradation.

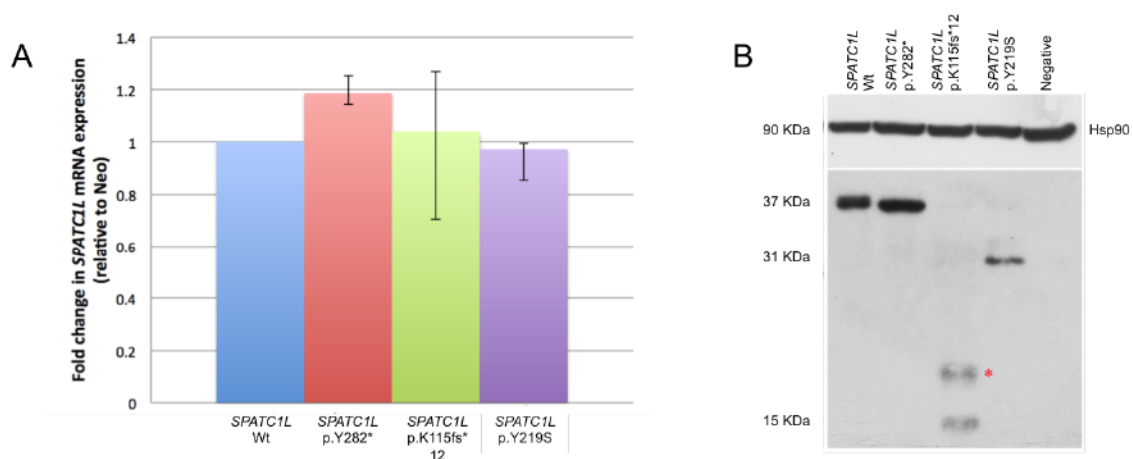


Figure 4.7 *SPATC1L* mRNA and protein levels in Hek293 transfected cells. (A) qRT-PCR analysis of relative mRNA expression of *SPATC1L* Wt and mutants after 48 hours of transfection in Hek 293 cells. Results are

expressed as a fold-change of expression levels, and are normalized to the relative amount of the internal standard Neo. Error bars indicate 95% confidence intervals. (B) Western Blot analysis of SPATC1L wt and mutants protein expression. Hsp90 was applied to determine equal loading.

In order to check the possible role of SPATC1L in the hearing system, gene expression was investigated in CD1 mice. These studies revealed the expression of *Spatc1l* (MGI: 1923823) in mouse whole cochlea. Expression level increases with age from P3 through P12, which corresponds to the development of the auditory perception, and then it remains stable until adult age (**Figure 4.8A**), suggesting its possible role in the development of the auditory system. Moreover, expression analysis on different tissues at 2 months of age highlighted a remarkable expression in both brain and testis (**Figure 4.6B**) suggesting a possible role also in these tissues, despite all cases here described do not present any clinical phenotype or laboratory finding related to this two tissues.

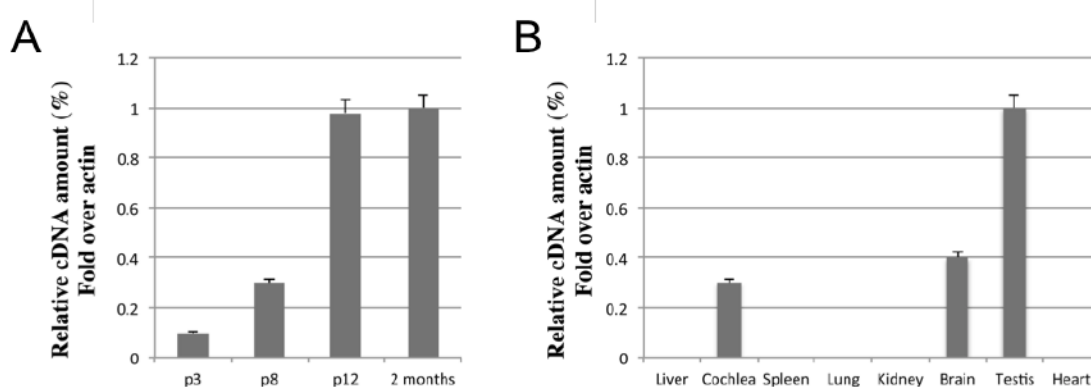


Figure 4.8. *Spatc1l* gene expression in mouse whole cochlea and other tissues at different time points. (A) The graph shows the expression of *Spatc1l* in mouse whole cochlea at P3, P8, P12 and 2 months. Results are reported as fold change in gene expression over β -actin, used as an internal control. The gene shows an age-related expression. (B) The graph shows *Spatc1l* gene expression at 2 months of age in different mouse tissues, including liver, cochlea, spleen, lung, kidney, brain, testis and heart. Results are reported as fold change in gene expression over β -actin, used as an internal control.

It remains to elucidate how exactly different mutations can lead to different phenotypes. In the case of HHL, a new nonsense mutation has been identified. Considering the preliminary results of our *in vitro* experiments, the mechanism of nonsense mRNA mediated decay is an unlikely event, however the generation of truncated protein isoforms may highly affect its

structure and localization, leading to an abnormal protein function. Moreover, the mutation involves both isoforms of the gene most likely leading to deleterious consequences. Accordingly, a similar severe phenotype was present in the ARHL patient carrying another disruptive allele (i.e. the frameshift insertion) despite affecting the coding region of only one of the two isoforms. As expected a milder phenotype is due to the presence of a missense mutation in the second ARHL patient.

Altogether these results suggest a role of *SPATC1L* gene in both hearing function and loss.

4.3.1 *PLS1*

A second Italian ADNSHL family (Figure 4.9A) showing a moderately severe to profound high frequencies hearing impairment (Figure 4.9B) was analysed by WES.

In particular, subjects II:2, II:3, II:4, II:5 and III:1 were selected for sequencing.

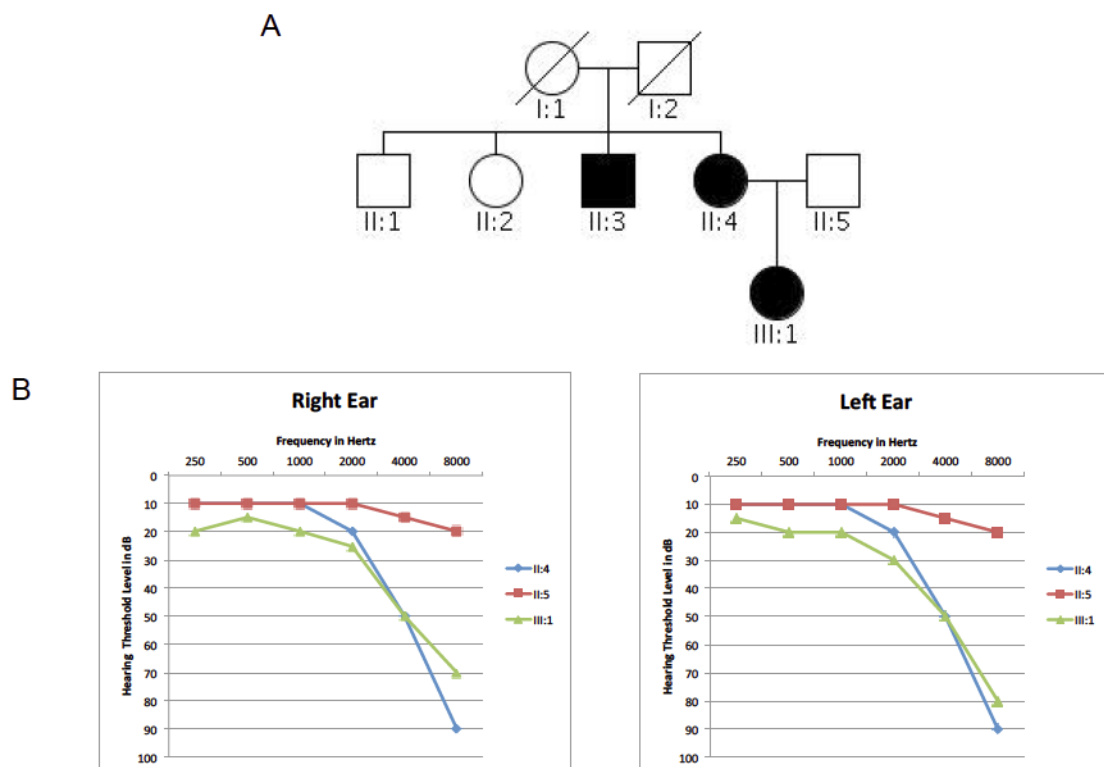


Figure 4.9 Pedigree and clinical features of the family. (A) Pedigree of the Italian family carrying the mutation in *PLS1* gene. Filled symbols represent affected. (B) Audiometric features of the individuals II:4, II:5 and III:1 displayed as audiograms (air conduction) and showing the thresholds of the right and left ears.

The overall mean-depth base coverage for WES was 99X, while on average 92% of the targeted region was covered at least 20-fold. A total of 83.412 genetic variants were called among the five subjects included in WES study. After data filtering, 6 candidate missense variants remained. These have been prioritized according to the role of the gene based on literature research. Three missense variants affecting genes associated to specific phenotypes not present in any of our patients were excluded (i.e. *MC1R* associated to Analgesia from kappa-opioid receptor agonist, female-specific (OMIM 613098), Skin/hair/eye pigmentation 2, blond/red hair/fair skin, UV-induced skin damage (OMIM 266300), Albinism, oculocutaneous, type II, modifier (OMIM 203200), Melanoma, cutaneous malignant, 5 (OMIM 613099); *ALOXE3* associated to Ichthyosis, congenital, autosomal recessive 3 (OMIM 606545); *PGAM2* associated to Glycogen storage disease X (OMIM 261670)). Among the remaining SNVs, one involves a gene of unknown function, *C14orf132*, which has been recently proposed as a candidate for pre and early postnatal developmental delay (130), another one involved *AVL9* gene that is a cancer driver candidate gene (131) and the last one affects *PLS1* gene that has recently been described as causative of HL in mouse (132). Taking into account these data, the *PLS1* mutation identified through WES was considered as causative.

The c.G805A (NM_001145319, ENST00000457734.6) variant, never described in any public database and predicted as causative by all *in silico* predictor tools, causes the amino acidic substitution p.E269K, which interests a highly conserved residue, according to PhyloP score (**Figure 4.10A**).

pronephros (**Figure 4.11B**). Images on transverse sections focus on different anteroposterior regions of the inner ear (outlined with White dotted line; **Figure 4.11C-E''**). *Pls1* is detected at hair cells (**Figure 4.11C,D,E**), as seen by its colocalization with GFP (**Figure 4.11C'',D'',E''**), which is activated specifically on that cell population through the *brn3c* promoter (**Figure 4.11C',D',E'**).

PLS1

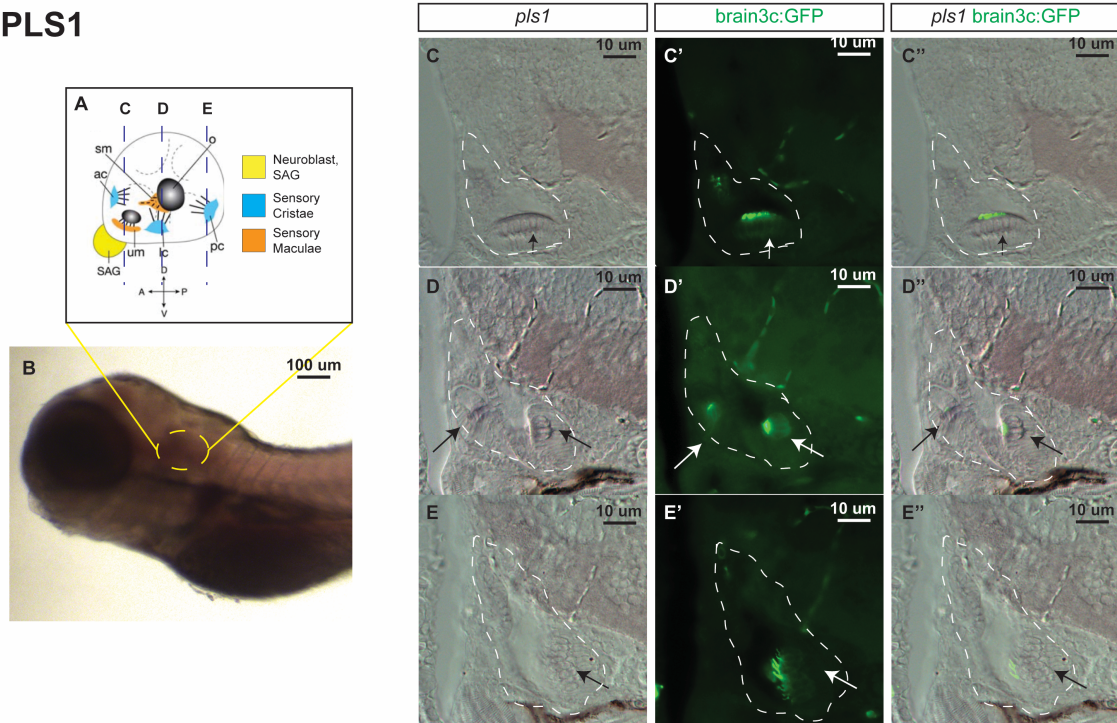


Figure 4.11 *Pls1* expression in Zebrafish larvae. (A) Schematic of 5 dpf inner ear cellular organization. Position of transversal views (C,D,E) are outlined by dotted lines. (B) Lateral view of anterior region of the 5 dpf larvae. Yellow circle delimit the inner ear location. C,C',C'') Transversal view of anterior region of inner ear. Inner ear is outlined by a white dotted line. Arrows point to hair cell patches location. (C) *Pls1* ISH. (C') *brain3c:GFP*. (C'') *Pls1* and *brain3c:GFP* merge image. (D,D',D'') Transversal view of medial region of inner ear. Inner ear is outlined by a white dotted line. Arrows point to hair cell patches location. (D) *Pls1* ISH. (D') *brain3c:GFP*. (D'') *Pls1* and *brain3c:GFP* merge image. (E,E',E'') Transversal view of medial region of inner ear. Inner ear is outlined by a white dotted line. Arrows point to hair cell patches location. (E) *Pls1* ISH. (E') *brain3c:GFP*. (E'') *Pls1* and *brain3c:GFP* merge image.

These findings (i.e. the identification of a pathogenic *PLS1* variant as the only probable cause of NSHL in an Italian family, the involvement of this gene in the etiopathogenesis of hearing loss in mouse, and the characteristic expression pattern in Zebrafish inner ear)

highly support the possible causative role *PLS1* in NSHL in humans. The Zebrafish knock-in model is now in progress and will help in elucidating the role of the p.E269K mutation.

5. CONCLUSIONS

The development and application of a multi-step strategy based on TRS and WES has proved to be an extremely powerful tool for the molecular diagnosis of NSHL.

As regards TRS, a custom sequencing panel of 96 deafness-genes has been applied to 32 Italian and 18 Qatari families, and allowed us to reach an overall detection rate of 50%.

An effective molecular diagnosis is a real benefit for genetic counselling, for the definition of the recurrence risk, prognosis and eventually therapeutic options.

Interestingly thanks to the use of our TRS panel, in some cases it has been possible to define a proper diagnosis, even before the appearance of clinical symptoms. This is what happened with a family diagnosed with NSHL, that however carried two missense mutations in *MYO7A* associated to Usher syndrome type 1b, or with a family carrying a *STRC-CATSPER2* deletion, associated to deafness-infertility syndrome (DIS) in males. It is worthless to say that these findings effectively impacted on the clinical management of patients.

As expected, TRS results highlighted a higher genetic heterogeneity in the Italian population compared to the Qatari one, where a single *CDH23* allele has been identified as a major player. The identification of mutations/genes affecting more families is really important for the definition of correct genotype/phenotype correlations that may help clinicians in foreseeing the molecular diagnosis. Moreover, considering all the recent advances in the field of genome editing and gene therapy, the detection of a common major player may be the base for the development of a population-specific gene therapy.

Interestingly in both Italian and Qatari populations two large CNVs involving *STRC/CATSPER2* and *OTOA* were detected, highlighting the importance of CNV analysis in HL patients.

After TRS it was not possible to define a clear molecular cause in half of patients. This result may be explained in different ways:

- 1) The causative gene is not included in the TRS panel,
- 2) The mutation lies in exons that are missing from the used reference assembly (GRCh37),
- 3) The mutation lies in regions not covered by the TRS panel, or in regions with low coverage,
- 4) The mutation is located in intronic regions.

Some of these issues may be overcome with whole exome sequencing, thus families negative to TRS were selected for WES.

As a first step, only families with well-defined phenotypes were sequenced.

So far, WES led to the discovery of two strong candidate genes: *SPATC1L* and *PLS1* in two Italian ADNSHL families, while data analysis of 11 other families is now in progress.

In order to definitely prove the pathogenic role of these genes several functional studies are needed. Some of them have already been performed via both *in vitro* and *in vivo* approaches that strengthened the hypothesis of their involvement in the onset of NSHL.

The identification of new NSHL-genes is essential for understanding the molecular biology of the hearing system and for guaranteeing a proper diagnosis in a bigger percentage of patients. Moreover, the identification of new genes will definitely help in the development of new therapeutic approaches, moving forward to a personalised medicine.

As in the case of TRS, any negative result after WES analysis could be explained by mutations affecting regions missing from the used reference assembly, or not covered by the exome enrichment kit, or poorly covered. Moreover the phenotype may be caused by deep intronic variants or structural variants, not detectable neither with TRS or WES. In order to overcome these limits, whole genome sequencing (WGS) may represent the most suitable alternative.

Despite the limits of both TRS and WES, our results proved that the combination of these technologies, together with functional experiments, could effectively enhance, in a cost effective way, the genetic characterization of NSHI/NSHL affected families.

6. REFERENCES

1. Anthwal,N. and Thompson,H. (2016) The development of the mammalian outer and middle ear. *J. Anat.*, **228**, 217–32.
2. Maier,W. and Ruf,I. (2016) Evolution of the mammalian middle ear: a historical review. *J. Anat.*, **228**, 270–83.
3. Fuchs,J.C. and Tucker,A.S. (2015) Development and Integration of the Ear. *Curr. Top. Dev. Biol.*, **115**, 213–32.
4. Nin,F., Yoshida,T., Sawamura,S., Ogata,G., Ota,T., Higuchi,T., Murakami,S., Doi,K., Kurachi,Y. and Hibino,H. (2016) The unique electrical properties in an extracellular fluid of the mammalian cochlea; their functional roles, homeostatic processes, and pathological significance. *Pflugers Arch.*, **468**, 1637–49.
5. VON BEKESY,G. (1952) Resting potentials inside the cochlear partition of the guinea pig. *Nature*, **169**, 241–2.
6. Goutman,J.D., Elgoyhen,A.B. and Gómez-Casati,M.E. (2015) Cochlear hair cells: The sound-sensing machines. *FEBS Lett.*, **589**, 3354–61.
7. Mann,Z.F. and Kelley,M.W. (2011) Development of tonotopy in the auditory periphery. *Hear. Res.*, **276**, 2–15.
8. Pepermans,E. and Petit,C. (2015) The tip-link molecular complex of the auditory mechano-electrical transduction machinery. *Hear. Res.*, **330**, 10–7.
9. Fettiplace,R. and Kim,K.X. (2014) The physiology of mechanoelectrical transduction channels in hearing. *Physiol. Rev.*, **94**, 951–86.
10. Coate,T.M. and Kelley,M.W. (2013) Making connections in the inner ear: recent insights into the development of spiral ganglion neurons and their connectivity with sensory hair cells. *Semin. Cell Dev. Biol.*, **24**, 460–9.
11. Ječmenica,J., Bajec-Opančina,A. and Ječmenica,D. (2015) Genetic hearing impairment. *Childs. Nerv. Syst.*, **31**, 515–9.
12. Smith,R.J., Shearer,A.E., Hildebrand,M.S. and Camp,G. Van (2014) Deafness and Hereditary Hearing Loss Overview.
13. Dror,A.A. and Avraham,K.B. (2009) Hearing Loss: Mechanisms Revealed by Genetics and Cell Biology. *Annu. Rev. Genet.*, **43**, 411–437.

14. Rehm,H.L. and Morton,C.C. (1999) A new age in the genetics of deafness. *Genet. Med. Off. J. Am. Coll. Med. Genet.*, **1**, 295–302; quiz 303.
15. Alford,R.L., Arnos,K.S., Fox,M., Lin,J.W., Palmer,C.G., Pandya,A., Rehm,H.L., Robin,N.H., Scott,D.A. and Yoshinaga-Itano,C. (2014) American College of Medical Genetics and Genomics guideline for the clinical evaluation and etiologic diagnosis of hearing loss. *Genet. Med. Off. J. Am. Coll. Med. Genet.*, **16**, 347–355.
16. Parker,M. and Bitner-Glindzicz,M. (2015) Genetic investigations in childhood deafness. *Arch. Dis. Child.*, **100**, 271–8.
17. Nishio,S. -y., Hattori,M., Moteki,H., Tsukada,K., Miyagawa,M., Naito,T., Yoshimura,H., Iwasa,Y. -i., Mori,K., Shima,Y., *et al.* (2015) Gene Expression Profiles of the Cochlea and Vestibular Endorgans: Localization and Function of Genes Causing Deafness. *Ann. Otol. Rhinol. Laryngol.*, **124**, 6S–48S.
18. Petit,C. and Weil,D. (2003) Deafness. In *Encyclopedia of Life Sciences*. John Wiley & Sons, Ltd, Chichester, UK.
19. Stelma,F. and Bhutta,M.F. (2014) Non-syndromic hereditary sensorineural hearing loss: review of the genes involved. *J. Laryngol. Otol.*, **128**, 13–21.
20. Venkatesh,M.D., Moorchung,N. and Puri,B. (2015) Genetics of non syndromic hearing loss. *Med. journal, Armed Forces India*, **71**, 363–8.
21. Egilmez,O.K. and Kalcioglu,M.T. (2016) Genetics of Nonsyndromic Congenital Hearing Loss. *Scientifica (Cairo).*, **2016**, 7576064.
22. Wilcox,E.R., Burton,Q.L., Naz,S., Riazuddin,S., Smith,T.N., Ploplis,B., Belyantseva,I., Ben-Yosef,T., Liburd,N.A., Morell,R.J., *et al.* (2001) Mutations in the gene encoding tight junction claudin-14 cause autosomal recessive deafness DFNB29. *Cell*, **104**, 165–72.
23. Riazuddin,S., Ahmed,Z.M., Fanning,A.S., Lagziel,A., Kitajiri,S., Ramzan,K., Khan,S.N., Chattaraj,P., Friedman,P.L., Anderson,J.M., *et al.* (2006) Tricellulin is a tight-junction protein necessary for hearing. *Am. J. Hum. Genet.*, **79**, 1040–51.
24. Walsh,T., Pierce,S.B., Lenz,D.R., Brownstein,Z., Dagan-Rosenfeld,O., Shahin,H., Roeb,W., McCarthy,S., Nord,A.S., Gordon,C.R., *et al.* (2010) Genomic duplication and overexpression of TJP2/ZO-2 leads to altered expression of apoptosis genes in progressive nonsyndromic hearing loss DFNA51. *Am. J. Hum. Genet.*, **87**, 101–9.
25. Forge,A., Becker,D., Casalotti,S., Edwards,J., Evans,W.H., Lench,N. and Souter,M. (1999) Gap junctions and connexin expression in the inner ear. *Novartis Found. Symp.*, **219**,

134-50–6.

26. Zonta,F., Buratto,D., Cassini,C., Bortolozzi,M. and Mammano,F. (2014) Molecular dynamics simulations highlight structural and functional alterations in deafness-related M34T mutation of connexin 26. *Front. Physiol.*, **5**, 85.
27. Rabionet,R., Gasparini,P. and Estivill,X. (2000) Molecular genetics of hearing impairment due to mutations in gap junction genes encoding beta connexins. *Hum. Mutat.*, **16**, 190–202.
28. Chan,D.K. and Chang,K.W. (2014) GJB2-associated hearing loss: systematic review of worldwide prevalence, genotype, and auditory phenotype. *Laryngoscope*, **124**, E34-53.
29. Liu,X.-Z., Yuan,Y., Yan,D., Ding,E.H., Ouyang,X.M., Fei,Y., Tang,W., Yuan,H., Chang,Q., Du,L.L., *et al.* (2009) Digenic inheritance of non-syndromic deafness caused by mutations at the gap junction proteins Cx26 and Cx31. *Hum. Genet.*, **125**, 53–62.
30. Abdelfatah,N., McComiskey,D.A., Doucette,L., Griffin,A., Moore,S.J., Negrijn,C., Hodgkinson,K.A., King,J.J., Larijani,M., Houston,J., *et al.* (2013) Identification of a novel in-frame deletion in KCNQ4 (DFNA2A) and evidence of multiple phenocopies of unknown origin in a family with ADSNHL. *Eur. J. Hum. Genet.*, **21**, 1112–9.
31. Schultz,J.M., Yang,Y., Caride,A.J., Filoteo,A.G., Penheiter,A.R., Lagziel,A., Morell,R.J., Mohiddin,S.A., Fananapazir,L., Madeo,A.C., *et al.* (2005) Modification of human hearing loss by plasma-membrane calcium pump PMCA2. *N. Engl. J. Med.*, **352**, 1557–64.
32. Riazuddin,S., Anwar,S., Fischer,M., Ahmed,Z.M., Khan,S.Y., Janssen,A.G.H., Zafar,A.U., Scholl,U., Husnain,T., Belyantseva,I.A., *et al.* (2009) Molecular basis of DFNB73: mutations of BSND can cause nonsyndromic deafness or Bartter syndrome. *Am. J. Hum. Genet.*, **85**, 273–80.
33. Dai,P., Stewart,A.K., Chebib,F., Hsu,A., Rozenfeld,J., Huang,D., Kang,D., Lip,V., Fang,H., Shao,H., *et al.* (2009) Distinct and novel SLC26A4/Pendrin mutations in Chinese and U.S. patients with nonsyndromic hearing loss. *Physiol. Genomics*, **38**, 281–90.
34. McGrath,J., Roy,P. and Perrin,B.J. (2016) Stereocilia morphogenesis and maintenance through regulation of actin stability. *Semin. Cell Dev. Biol.*, 10.1016/j.semcdb.2016.08.017.
35. Ebermann,I., Scholl,H.P.N., Charbel Issa,P., Becirovic,E., Lamprecht,J., Jurklics,B., Millán,J.M., Aller,E., Mitter,D. and Bolz,H. (2007) A novel gene for Usher syndrome type 2: mutations in the long isoform of whirlin are associated with retinitis pigmentosa and

- sensorineural hearing loss. *Hum. Genet.*, **121**, 203–11.
36. Tlili,A., Charfedine,I., Lahmar,I., Benzina,Z., Mohamed,B.A., Weil,D., Idriss,N., Drira,M., Masmoudi,S. and Ayadi,H. (2005) Identification of a novel frameshift mutation in the DFNB31/WHRN gene in a Tunisian consanguineous family with hereditary non-syndromic recessive hearing loss. *Hum. Mutat.*, **25**, 503.
 37. Ahmed,Z.M., Riazuddin,S., Riazuddin,S. and Wilcox,E.R. (2003) The molecular genetics of Usher syndrome. *Clin. Genet.*, **63**, 431–44.
 38. Ouyang,X.M., Xia,X.J., Verpy,E., Du,L.L., Pandya,A., Petit,C., Balkany,T., Nance,W.E. and Liu,X.Z. (2002) Mutations in the alternatively spliced exons of USH1C cause non-syndromic recessive deafness. *Hum. Genet.*, **111**, 26–30.
 39. Verpy,E., Leibovici,M., Michalski,N., Goodyear,R.J., Houdon,C., Weil,D., Richardson,G.P. and Petit,C. (2011) Stereocilin connects outer hair cell stereocilia to one another and to the tectorial membrane. *J. Comp. Neurol.*, **519**, 194–210.
 40. Zheng,J., Miller,K.K., Yang,T., Hildebrand,M.S., Shearer,A.E., DeLuca,A.P., Scheetz,T.E., Drummond,J., Scherer,S.E., Legan,P.K., *et al.* (2011) Carcinoembryonic antigen-related cell adhesion molecule 16 interacts with alpha-tectorin and is mutated in autosomal dominant hearing loss (DFNA4). *Proc. Natl. Acad. Sci. U. S. A.*, **108**, 4218–23.
 41. Zwaenepoel,I., Mustapha,M., Leibovici,M., Verpy,E., Goodyear,R., Liu,X.Z., Nouaille,S., Nance,W.E., Kanaan,M., Avraham,K.B., *et al.* (2002) Otoancorin, an inner ear protein restricted to the interface between the apical surface of sensory epithelia and their overlying acellular gels, is defective in autosomal recessive deafness DFNB22. *Proc. Natl. Acad. Sci. U. S. A.*, **99**, 6240–5.
 42. Ruel,J., Emery,S., Nouvian,R., Bersot,T., Amilhon,B., Van Rybroek,J.M., Rebillard,G., Lenoir,M., Eybalin,M., Delprat,B., *et al.* (2008) Impairment of SLC17A8 encoding vesicular glutamate transporter-3, VGLUT3, underlies nonsyndromic deafness DFNA25 and inner hair cell dysfunction in null mice. *Am. J. Hum. Genet.*, **83**, 278–92.
 43. Santarelli,R., del Castillo,I., Cama,E., Scimemi,P. and Starr,A. (2015) Audibility, speech perception and processing of temporal cues in ribbon synaptic disorders due to OTOF mutations. *Hear. Res.*, **330**, 200–12.
 44. Morín,M., Bryan,K.E., Mayo-Merino,F., Goodyear,R., Mencía,A., Modamio-Høybjør,S., del Castillo,I., Cabalka,J.M., Richardson,G., Moreno,F., *et al.* (2009) In vivo and in vitro effects of two novel gamma-actin (ACTG1) mutations that cause DFNA20/26 hearing

- impairment. *Hum. Mol. Genet.*, **18**, 3075–89.
45. Kitajiri,S., Sakamoto,T., Belyantseva,I.A., Goodyear,R.J., Stepanyan,R., Fujiwara,I., Bird,J.E., Riazuddin,S., Riazuddin,S., Ahmed,Z.M., *et al.* (2010) Actin-bundling protein TRIOBP forms resilient rootlets of hair cell stereocilia essential for hearing. *Cell*, **141**, 786–98.
 46. Rehman,A.U., Morell,R.J., Belyantseva,I.A., Khan,S.Y., Boger,E.T., Shahzad,M., Ahmed,Z.M., Riazuddin,S., Khan,S.N., Riazuddin,S., *et al.* (2010) Targeted capture and next-generation sequencing identifies C9orf75, encoding taperin, as the mutated gene in nonsyndromic deafness DFNB79. *Am. J. Hum. Genet.*, **86**, 378–88.
 47. Lynch,E.D., Lee,M.K., Morrow,J.E., Welcsh,P.L., León,P.E. and King,M.C. (1997) Nonsyndromic deafness DFNA1 associated with mutation of a human homolog of the *Drosophila* gene diaphanous. *Science*, **278**, 1315–8.
 48. Schraders,M., Haas,S.A., Weegerink,N.J.D., Oostrik,J., Hu,H., Hoefsloot,L.H., Kannan,S., Huygen,P.L.M., Pennings,R.J.E., Admiraal,R.J.C., *et al.* (2011) Next-generation sequencing identifies mutations of SMPX, which encodes the small muscle protein, X-linked, as a cause of progressive hearing impairment. *Am. J. Hum. Genet.*, **88**, 628–34.
 49. Raz-Prag,D., Zeng,Y., Sieving,P.A. and Bush,R.A. (2009) Photoreceptor protection by adeno-associated virus-mediated LEDGF expression in the RCS rat model of retinal degeneration: probing the mechanism. *Invest. Ophthalmol. Vis. Sci.*, **50**, 3897–906.
 50. Donaudy,F., Zheng,L., Ficarella,R., Ballana,E., Carella,M., Melchionda,S., Estivill,X., Bartles,J.R. and Gasparini,P. (2006) Espin gene (ESPN) mutations associated with autosomal dominant hearing loss cause defects in microvillar elongation or organisation. *J. Med. Genet.*, **43**, 157–61.
 51. Kitajiri,S., Fukumoto,K., Hata,M., Sasaki,H., Katsuno,T., Nakagawa,T., Ito,J., Tsukita,S. and Tsukita,S. (2004) Radixin deficiency causes deafness associated with progressive degeneration of cochlear stereocilia. *J. Cell Biol.*, **166**, 559–70.
 52. Okoruwa,O.E., Weston,M.D., Sanjeevi,D.C., Millemon,A.R., Fritzsche,B., Hallworth,R. and Beisel,K.W. Evolutionary insights into the unique electromotility motor of mammalian outer hair cells. *Evol. Dev.*, **10**, 300–15.
 53. Liu,X.Z., Ouyang,X.M., Xia,X.J., Zheng,J., Pandya,A., Li,F., Du,L.L., Welch,K.O., Petit,C., Smith,R.J.H., *et al.* (2003) Prestin, a cochlear motor protein, is defective in non-syndromic hearing loss. *Hum. Mol. Genet.*, **12**, 1155–62.

54. Hilgert,N., Smith,R.J.H. and Van Camp,G. (2009) Function and expression pattern of nonsyndromic deafness genes. *Curr. Mol. Med.*, **9**, 546–64.
55. Sommen,M., Schrauwen,I., Vandeweyer,G., Boeckx,N., Corneveaux,J.J., van den Ende,J., Boudewyns,A., De Leenheer,E., Janssens,S., Claes,K., *et al.* (2016) DNA Diagnostics of Hereditary Hearing Loss: A Targeted Resequencing Approach Combined with a Mutation Classification System. *Hum. Mutat.*, **37**, 812–819.
56. Yan,D., Tekin,M., Blanton,S.H. and Liu,X.Z. (2013) Next-generation sequencing in genetic hearing loss. *Genet. Test. Mol. Biomarkers*, **17**, 581–7.
57. Shearer,A.E. and Smith,R.J.H. (2015) Massively Parallel Sequencing for Genetic Diagnosis of Hearing Loss: The New Standard of Care. *Otolaryngol. Head. Neck Surg.*, **153**, 175–82.
58. Samorodnitsky,E., Jewell,B.M., Hagopian,R., Miya,J., Wing,M.R., Lyon,E., Damodaran,S., Bhatt,D., Reeser,J.W., Datta,J., *et al.* (2015) Evaluation of Hybridization Capture Versus Amplicon-Based Methods for Whole-Exome Sequencing. *Hum. Mutat.*, **36**, 903–14.
59. Lin,X., Tang,W., Ahmad,S., Lu,J., Colby,C.C., Zhu,J. and Yu,Q. (2012) Applications of targeted gene capture and next-generation sequencing technologies in studies of human deafness and other genetic disabilities. *Hear. Res.*, **288**, 67–76.
60. Shearer,A.E., Hildebrand,M.S., Sloan,C.M. and Smith,R.J.H. (2011) Deafness in the genomics era. *Hear. Res.*, **282**, 1–9.
61. Tekin,D., Yan,D., Bademci,G., Feng,Y., Guo,S., Foster,J., Blanton,S., Tekin,M. and Liu,X. (2016) A next-generation sequencing gene panel (MiamiOtoGenes) for comprehensive analysis of deafness genes. *Hear. Res.*, **333**, 179–84.
62. Friedman,T.B. and Griffith,A.J. (2003) Human nonsyndromic sensorineural deafness. *Annu. Rev. Genomics Hum. Genet.*, **4**, 341–402.
63. Atik,T., Bademci,G., Diaz-Horta,O., Blanton,S.H. and Tekin,M. (2015) Whole-exome sequencing and its impact in hereditary hearing loss. *Genet. Res. (Camb)*, **97**, e4.
64. Khalifa Alkowari,M., Giroto,G., Abdulhadi,K., Dipresa,S., Siam,R., Najjar,N., Badii,R. and Gasparini,P. (2012) GJB2 and GJB6 genes and the A1555G mitochondrial mutation are only minor causes of nonsyndromic hearing loss in the Qatari population. *Int. J. Audiol.*, **51**, 181–5.
65. Clark,J.G. (1981) Uses and abuses of hearing loss classification. *ASHA*, **23**, 493–500.
66. Vozzi,D., Morgan,A., Vuckovic,D., D'Eustacchio,A., Abdulhadi,K., Rubinato,E., Badii,R.,

- Gasparini,P. and Girotto,G. (2014) Hereditary hearing loss: a 96 gene targeted sequencing protocol reveals novel alleles in a series of Italian and Qatari patients. *Gene*, **542**, 209–16.
67. Valle Giorgio CRIBI Genomics and Bioinformatics.
68. Danecek,P., Auton,A., Abecasis,G., Albers,C.A., Banks,E., DePristo,M.A., Handsaker,R.E., Lunter,G., Marth,G.T., Sherry,S.T., *et al.* (2011) The variant call format and VCFtools. *Bioinformatics*, **27**, 2156–2158.
69. Wang,K., Li,M. and Hakonarson,H. (2010) ANNOVAR: functional annotation of genetic variants from high-throughput sequencing data. *Nucleic Acids Res.*, **38**, e164–e164.
70. Adzhubei,I., Jordan,D.M. and Sunyaev,S.R. (2013) Predicting functional effect of human missense mutations using PolyPhen-2. *Curr. Protoc. Hum. Genet.*, **Chapter 7**, Unit7.20.
71. Ng,P.C. and Henikoff,S. (2003) SIFT: Predicting amino acid changes that affect protein function. *Nucleic Acids Res.*, **31**, 3812–4.
72. Schwarz,J.M., Rödelberger,C., Schuelke,M. and Seelow,D. (2010) MutationTaster evaluates disease-causing potential of sequence alterations. *Nat. Methods*, **7**, 575–6.
73. Chun,S. and Fay,J.C. (2009) Identification of deleterious mutations within three human genomes. *Genome Res.*, **19**, 1553–1561.
74. Kircher,M., Witten,D.M., Jain,P., O’Roak,B.J., Cooper,G.M. and Shendure,J. (2014) A general framework for estimating the relative pathogenicity of human genetic variants. *Nat. Genet.*, **46**, 310–5.
75. Pollard,K.S., Hubisz,M.J., Rosenbloom,K.R. and Siepel,A. (2010) Detection of nonneutral substitution rates on mammalian phylogenies. *Genome Res.*, **20**, 110–21.
76. Cooper,G.M., Stone,E.A., Asimenos,G., NISC Comparative Sequencing Program, Green,E.D., Batzoglou,S. and Sidow,A. (2005) Distribution and intensity of constraint in mammalian genomic sequence. *Genome Res.*, **15**, 901–13.
77. Desmet,F.-O., Hamroun,D., Lalande,M., Collod-Beroud,G., Claustres,M. and Beroud,C. (2009) Human Splicing Finder: an online bioinformatics tool to predict splicing signals. *Nucleic Acids Res.*, **37**, e67–e67.
78. Thorvaldsdottir,H., Robinson,J.T. and Mesirov,J.P. (2013) Integrative Genomics Viewer (IGV): high-performance genomics data visualization and exploration. *Brief. Bioinform.*, **14**, 178–192.
79. Johansson,L.F., van Dijk,F., de Boer,E.N., van Dijk-Bos,K.K., Jongbloed,J.D.H., van der

- Hout,A.H., Westers,H., Sinke,R.J., Swertz,M.A., Sijmons,R.H., *et al.* (2016) CoNVaDING: Single Exon Variation Detection in Targeted NGS Data. *Hum. Mutat.*, **37**, 457–464.
80. Harrison,O.J., Jin,X., Hong,S., Bahna,F., Ahlsen,G., Brasch,J., Wu,Y., Vendome,J., Felsovalyi,K., Hampton,C.M., *et al.* (2011) The Extracellular Architecture of Adherens Junctions Revealed by Crystal Structures of Type I Cadherins. *Structure*, **19**, 244–256.
81. Brunner,J.D., Lim,N.K., Schenck,S., Duerst,A. and Dutzler,R. (2014) X-ray structure of a calcium-activated TMEM16 lipid scramblase. *Nature*, **516**, 207–212.
82. Benkert,P., Biasini,M. and Schwede,T. (2011) Toward the estimation of the absolute quality of individual protein structure models. *Bioinformatics*, **27**, 343–350.
83. Gajendrarao,P., Krishnamoorthy,N., Kassem,H.S., Moharem-Elgamal,S., Cecchi,F., Olivotto,I. and Yacoub,M.H. (2013) Molecular Modeling of Disease Causing Mutations in Domain C1 of cMyBP-C. *PLoS One*, **8**, e59206.
84. Yang,J. and Zhang,Y. (2015) Protein Structure and Function Prediction Using I-TASSER. *Curr. Protoc. Bioinforma.*, **52**, 5.8.1-15.
85. Van Der Spoel,D., Lindahl,E., Hess,B., Groenhof,G., Mark,A.E. and Berendsen,H.J.C. (2005) GROMACS: Fast, flexible, and free. *J. Comput. Chem.*, **26**, 1701–1718.
86. Hess,B., Kutzner,C., Van Der Spoel,D. and Lindahl,E. (2008) GROMACS 4: Algorithms for Highly Efficient, Load-Balanced, and Scalable Molecular Simulation. *J. Chem. Theory Comput*, **4**, 435–447.
87. Stocker,U. and van Gunsteren,W.F. (2000) Molecular dynamics simulation of hen egg white lysozyme: a test of the GROMOS96 force field against nuclear magnetic resonance data. *Proteins*, **40**, 145–53.
88. Berendsen,H.J.C., Postma,J.P.M., Van Gunsteren,W.F. and Hermans,J. INTERACTION MODELS FOR WATER IN RELATION TO PROTEIN HYDRATION.
89. Hess,B., Bekker,H., Berendsen,H.J.C. and Fraaije,J.G.E.M. (1997) 3 LINCS: a linear constraint solver for molecular simulations. *Chem*, **18**, 1463–1472.
90. Miyamoto,S. and Kollman,P.A. (1992) Settle: An analytical version of the SHAKE and RATTLE algorithm for rigid water models. *J. Comput. Chem.*, **13**, 952–962.
91. Berendsen,H.J.C., Postma,J.P.M., van Gunsteren,W.F., DiNola,A. and Haak,J.R. (1984) Molecular dynamics with coupling to an external bath. *J. Chem. Phys.*, **81**, 3684–3690.
92. Kingston,R.E., Chen,C.A., Rose,J.K., Kingston,R.E., Chen,C.A. and Rose,J.K. (2003) Calcium Phosphate Transfection. In *Current Protocols in Molecular Biology*. John Wiley & Sons,

- Inc., Hoboken, NJ, USA, p. 9.1.1-9.1.11.
93. Livak, K.J. and Schmittgen, T.D. (2001) Analysis of relative gene expression data using real-time quantitative PCR and the 2(-Delta Delta C(T)) Method. *Methods*, **25**, 402–8.
 94. Nuovo, G.J. (2010) In situ detection of microRNAs in paraffin embedded, formalin fixed tissues and the co-localization of their putative targets. *Methods*, **52**, 307–315.
 95. Abe, S., Usami, S., Shinkawa, H., Kelley, P.M. and Kimberling, W.J. (2000) Prevalent connexin 26 gene (GJB2) mutations in Japanese. *J. Med. Genet.*, **37**, 41–3.
 96. Kelsell, D.P., Dunlop, J., Stevens, H.P., Lench, N.J., Liang, J.N., Parry, G., Mueller, R.F. and Leigh, I.M. (1997) Connexin 26 mutations in hereditary non-syndromic sensorineural deafness. *Nature*, **387**, 80–83.
 97. Vona, B., Hofrichter, M.A.H., Neuner, C., Schröder, J., Gehrig, A., Hennermann, J.B., Kraus, F., Shehata-Dieler, W., Klopocki, E., Nanda, I., *et al.* (2015) DFNB16 is a frequent cause of congenital hearing impairment: implementation of STRC mutation analysis in routine diagnostics. *Clin. Genet.*, **87**, 49–55.
 98. Bharadwaj, A.K., Kasztejna, J.P., Huq, S., Berson, E.L. and Dryja, T.P. (2000) Evaluation of the Myosin VIIA Gene and Visual Function in Patients with Usher Syndrome Type I. *Exp. Eye Res.*, **71**, 173–181.
 99. Donaudy, F., Snoeckx, R., Pfister, M., Zenner, H.-P., Blin, N., Di Stazio, M., Ferrara, A., Lanzara, C., Ficarella, R., Declau, F., *et al.* (2004) Nonmuscle Myosin Heavy-Chain Gene MYH14 Is Expressed in Cochlea and Mutated in Patients Affected by Autosomal Dominant Hearing Impairment (DFNA4). *Am. J. Hum. Genet.*, **74**, 770–776.
 100. Hildebrand, M.S., Morín, M., Meyer, N.C., Mayo, F., Modamio-Hoybjør, S., Mencía, A., Olavarrieta, L., Morales-Angulo, C., Nishimura, C.J., Workman, H., *et al.* (2011) DFNA8/12 caused by TECTA mutations is the most identified subtype of nonsyndromic autosomal dominant hearing loss. *Hum. Mutat.*, **32**, 825–834.
 101. Yuan, Y., Guo, W., Tang, J., Zhang, G., Wang, G., Han, M., Zhang, X., Yang, S., He, D.Z.Z., Dai, P., *et al.* (2012) Molecular Epidemiology and Functional Assessment of Novel Allelic Variants of SLC26A4 in Non-Syndromic Hearing Loss Patients with Enlarged Vestibular Aqueduct in China. *PLoS One*, **7**, e49984.
 102. Kalay, E., Karaguzel, A., Caylan, R., Heister, A., Cremers, F.P.M., Cremers, C.W.R.J., Brunner, H.G., de Brouwer, A.P.M. and Kremer, H. (2005) Four novel TMC1 (DFNB7/DFNB11) mutations in Turkish patients with congenital autosomal recessive

- nonsyndromic hearing loss. *Hum. Mutat.*, **26**, 591.
103. Rodríguez-Ballesteros,M., Reynoso,R., Olarte,M., Villamar,M., Morera,C., Santarelli,R., Arslan,E., Medá,C., Curet,C., Völter,C., *et al.* (2008) A multicenter study on the prevalence and spectrum of mutations in the otoferlin gene (*OTOF*) in subjects with nonsyndromic hearing impairment and auditory neuropathy. *Hum. Mutat.*, **29**, 823–831.
 104. Shahin,H., Walsh,T., Rayyan,A.A., Lee,M.K., Higgins,J., Dickel,D., Lewis,K., Thompson,J., Baker,C., Nord,A.S., *et al.* (2010) Five novel loci for inherited hearing loss mapped by SNP-based homozygosity profiles in Palestinian families. *Eur. J. Hum. Genet.*, **18**, 407–13.
 105. Khalifa Alkowari,M., Girotto,G., Abdulhadi,K., Dipresa,S., Siam,R., Najjar,N., Badii,R. and Gasparini,P. (2012) GJB2 and GJB6 genes and the A1555G mitochondrial mutation are only minor causes of nonsyndromic hearing loss in the Qatari population. *Int. J. Audiol.*, **51**, 181–185.
 106. Ma,Y., Xiao,Y., Zhang,F., Han,Y., Li,J., Xu,L., Bai,X. and Wang,H. (2016) Novel compound heterozygous mutations in MYO7A gene associated with autosomal recessive sensorineural hearing loss in a Chinese family. *Int. J. Pediatr. Otorhinolaryngol.*, **83**, 179–185.
 107. Lentz,J. and Keats,B.J. (1993) Usher Syndrome Type I.
 108. Di Leva,F., D’Adamo,P., Cubellis,M.V., D’Eustacchio,A., Errichiello,M., Saulino,C., Auletta,G., Giannini,P., Donaudy,F., Ciccodicola,A., *et al.* (2006) Identification of a novel mutation in the myosin VIIA motor domain in a family with autosomal dominant hearing loss (DFNA11). *Audiol. Neurotol.*, **11**, 157–64.
 109. Duman,D., Sirmaci,A., Cengiz,F.B., Ozdag,H. and Tekin,M. (2011) Screening of 38 genes identifies mutations in 62% of families with nonsyndromic deafness in Turkey. *Genet. Test. Mol. Biomarkers*, **15**, 29–33.
 110. Bork,J.M., Peters,L.M., Riazuddin,S., Bernstein,S.L., Ahmed,Z.M., Ness,S.L., Polomeno,R., Ramesh,A., Schloss,M., Srisailpathy,C.R., *et al.* (2001) Usher syndrome 1D and nonsyndromic autosomal recessive deafness DFNB12 are caused by allelic mutations of the novel cadherin-like gene CDH23. *Am. J. Hum. Genet.*, **68**, 26–37.
 111. Astuto,L.M., Bork,J.M., Weston,M.D., Askew,J.W., Fields,R.R., Orten,D.J., Ohliger,S.J., Riazuddin,S., Morell,R.J., Khan,S., *et al.* (2002) CDH23 mutation and phenotype

- heterogeneity: a profile of 107 diverse families with Usher syndrome and nonsyndromic deafness. *Am. J. Hum. Genet.*, **71**, 262–75.
112. De Keulenaer,S., Hellemans,J., Lefever,S., Renard,J.-P., De Schrijver,J., Van de Voorde,H., Tabatabaiefar,M.A., Van Nieuwerburgh,F., Flamez,D., Pattyn,F., *et al.* (2012) Molecular diagnostics for congenital hearing loss including 15 deafness genes using a next generation sequencing platform. *BMC Med. Genomics*, **5**, 17.
 113. Santos,R.L.P., Wajid,M., Khan,M.N., McArthur,N., Pham,T.L., Bhatti,A., Lee,K., Irshad,S., Mir,A., Yan,K., *et al.* (2005) Novel sequence variants in theTMC1 gene in Pakistani families with autosomal recessive hearing impairment. *Hum. Mutat.*, **26**, 396–396.
 114. Yang,T., Wei,X., Chai,Y., Li,L. and Wu,H. (2013) Genetic etiology study of the non-syndromic deafness in Chinese Hans by targeted next-generation sequencing. *Orphanet J. Rare Dis.*, **8**, 85.
 115. Bakhchane,A., Charoute,H., Nahili,H., Roky,R., Rouba,H., Charif,M., Lenaers,G. and Barakat,A. (2015) A novel mutation in the TMC1 gene causes non-syndromic hearing loss in a Moroccan family. *Gene*, **574**, 28–33.
 116. Shearer,A.E., Kolbe,D.L., Azaiez,H., Sloan,C.M., Frees,K.L., Weaver,A.E., Clark,E.T., Nishimura,C.J., Black-Ziegelbein,E.A. and Smith,R.J.H. (2014) Copy number variants are a common cause of non-syndromic hearing loss. *Genome Med.*, **6**, 37.
 117. Verpy,E., Masmoudi,S., Zwaenepoel,I., Leibovici,M., Hutchin,T.P., Del Castillo,I., Nouaille,S., Blanchard,S., Lainé,S., Popot,J.L., *et al.* (2001) Mutations in a new gene encoding a protein of the hair bundle cause non-syndromic deafness at the DFNB16 locus. *Nat. Genet.*, **29**, 345–9.
 118. Zhang,Y., Malekpour,M., Al-Madani,N., Kahrizi,K., Zanganeh,M., Mohseni,M., Mojahedi,F., Daneshi,A., Najmabadi,H. and Smith,R.J.H. (2009) Sensorineural deafness and male infertility: a contiguous gene deletion syndrome. *BMJ Case Rep.*, **2009**, bcr0820080645.
 119. Hoppman,N., Aypar,U., Brodersen,P., Brown,N., Wilson,J., Babovic-Vuksanovic,D., Morton,C., Nance,W., Zhang,Y., Malekpour,M., *et al.* (2013) Genetic testing for hearing loss in the United States should include deletion/duplication analysis for the deafness/infertility locus at 15q15.3. *Mol. Cytogenet.*, **6**, 19.
 120. Francey,L.J., Conlin,L.K., Kadesch,H.E., Clark,D., Berrodin,D., Sun,Y., Glessner,J., Hakonarson,H., Jalas,C., Landau,C., *et al.* (2012) Genome-wide SNP genotyping

- identifies the Stereocilin (STRC) gene as a major contributor to pediatric bilateral sensorineural hearing impairment. *Am. J. Med. Genet. A*, **158A**, 298–308.
121. Dostal,A., Nemeckova,J., Gaillyova,R., Vranova,V., Zezulkova,D., Lejska,M., Slapak,I., Dostalova,Z. and Kuglik,P. (2006) Identification of 2.3-Mb gene locus for congenital aural atresia in 18q22.3 deletion: a case report analyzed by comparative genomic hybridization. *Otol. Neurotol.*, **27**, 427–32.
 122. Masuda,T., Sakuma,C., Nagaoka,A., Yamagishi,T., Ueda,S., Nagase,T. and Yaginuma,H. (2014) Follistatin-like 5 is expressed in restricted areas of the adult mouse brain: Implications for its function in the olfactory system. *Congenit. Anom. (Kyoto)*, **54**, 63–6.
 123. Kingwell,K. (2011) FSTL5--a new prognostic biomarker for medulloblastoma. *Nat. Rev. Neurol.*, **7**, 598.
 124. Giroto,G., Pirastu,N., Gasparini,A., D'Adamo,P. and Gasparini,P. (2011) Frequency of hearing loss in a series of rural communities of five developing countries located along the Silk Road. *Audiol. Med.*, **9**, 135–140.
 125. Lecat,S., Matthes,H.W.D., Pepperkok,R., Simpson,J.C. and Galzi,J.-L. (2015) A Fluorescent Live Imaging Screening Assay Based on Translocation Criteria Identifies Novel Cytoplasmic Proteins Implicated in G Protein-coupled Receptor Signaling Pathways. *Mol. Cell. Proteomics*, **14**, 1385–99.
 126. Wingard,J.C. and Zhao,H.-B. (2015) Cellular and Deafness Mechanisms Underlying Connexin Mutation-Induced Hearing Loss - A Common Hereditary Deafness. *Front. Cell. Neurosci.*, **9**, 202.
 127. Zhao,H.-B. (2016) Expression and function of pannexins in the inner ear and hearing. *BMC Cell Biol.*, **17 Suppl 1**, 16.
 128. Fry,R.C., Svensson,J.P., Valiathan,C., Wang,E., Hogan,B.J., Bhattacharya,S., Bugni,J.M., Whittaker,C.A. and Samson,L.D. (2008) Genomic predictors of interindividual differences in response to DNA damaging agents. *Genes Dev.*, **22**, 2621–6.
 129. Fujimoto,C. and Yamasoba,T. (2014) Oxidative stresses and mitochondrial dysfunction in age-related hearing loss. *Oxid. Med. Cell. Longev.*, **2014**, 582849.
 130. Tiirats,A., Viltrop,T., Nõukas,M., Reimann,E., Salumets,A. and Kõks,S. (2016) C14orf132 gene is possibly related to extremely low birth weight. *BMC Genet.*, **17**, 132.
 131. Li,Y., Xu,J., Xiong,H., Ma,Z., Wang,Z., Kipreos,E.T., Dalton,S. and Zhao,S. (2014) Cancer driver candidate genes &AVL9&; &DENND5A&;

- and *NUPL1* contribute to MDCK cystogenesis. *Oncoscience*, **1**, 854.
132. Taylor,R., Bullen,A., Johnson,S.L., Grimm-Gunter,E.-M., Rivero,F., Marcotti,W., Forge,A. and Daudet,N. (2015) Absence of plastin 1 causes abnormal maintenance of hair cell stereocilia and a moderate form of hearing loss in mice. *Hum. Mol. Genet.*, **24**, 37–49.
133. Sjöblom,B., Ylänne,J. and Djinić-Carugo,K. (2008) Novel structural insights into F-actin-binding and novel functions of calponin homology domains. *Curr. Opin. Struct. Biol.*, **18**, 702–708.